Chapter 3

Correlations for two-qubit X-states

3.1 Introduction

The study of correlations in bipartite systems has been invigorated over the last couple of decades or so. Various measures and approaches to segregate the classical and quantum contents of correlations have been explored. Entanglement has continued to be the most popular of these correlations owing to its inherent potential advantages in performing quantum computation and communication tasks [181]. More recently, however, there has been a rapidly growing interest in the study of correlations from a more direct measurement perspective [65, 182], and several measures to quantify the same have been considered. Among these measures, quantum discord and classical correlation have been attracting much attention [183–188], and have lead to several interesting results [189–192]. There has also been recent studies of different aspects of correlations like their evolution in various systems [193–196], including non-markovian environments [197–200] and its role in spin systems [201, 202]. Methods of witnessing quantum discord in the theoretical [203–213] and experimental [214–218] domain have also been explored.

In this Chapter, we undertake a comprehensive analysis of the problem of computation of correlations in the two-qubit system, especially the so-called X-states of two-qubit

system [43]; this class of states has come to be accorded a distinguished status in this regard. The problem of X-states has already been considered in [219–225] and that of more general two-qubit states in [226–230]. The approach which we present here exploits the very *geometric nature* of the problem, and helps to clarify and correct some issues regarding computation of correlations in X-states in the literature, and many new insights emerge. It may be emphasised that the geometric methods used here have been the basic tools of (classical) polarization optics for a very long time, and involve constructs like Stokes vectors, Poincaré sphere, and Mueller matrices [231–235].

In Section 3.8 we compare our analysis and results with those of the well known work of Ali, Rau, and Alber [220]. We show that their famous theorem that the optimal POVM for X-states is always a von Neumann projection either along x or along the z direction holds numerically for the entire manifold of X-states except for a very tiny region. Perhaps surprisingly, however, *their symmetry-based proof of that theorem seems to make an a priori assumption equivalent to the theorem itself.*

3.2 Mueller-Stokes formalism for two-qubit states

We begin with a brief indication as to why the Mueller-Stokes formalism of classical optics is possibly the most appropriate one for handling quantum states post measurement. In classical polarization optics the state of a light beam is represented by a 2×2 complex positive matrix Φ called the *polarization matrix* [236]. The intensity of the beam is identified with $\mathrm{Tr}\,\Phi$, and so the matrix $(\mathrm{Tr}\,\Phi)^{-1}\Phi$ (normalized to unit trace) represents the actual *state* of polarization. The polarization matrix Φ is thus analogous to the density matrix of a qubit, the only distinction being that the trace of the latter needs to assume unit value. Even this one little difference is gone when one deals with *conditional quantum states* post measurement: the probability of obtaining a conditional state becomes analogous to intensity $= \mathrm{Tr}\,\Phi$ of the classical context.

The Mueller-Stokes formalism itself arises from the following simple fact : any 2×2 matrix Φ can be invertibly associated with a four-vector S, called the Stokes vector, through

$$\Phi = \frac{1}{2} \sum_{k=0}^{3} S_k \sigma_k, \quad S_k = \mathrm{Tr}(\sigma_k \Phi). \tag{3.1}$$

This representation is an immediate consequence of the fact that the Pauli triplet σ_1, σ_2, σ_3 and $\sigma_0 = \mathbb{1}$, the unit matrix, form a complete orthonormal set of (hermitian) matrices.

Clearly, hermiticity of the polarization matrix Φ is *equivalent* to reality of the associated four-vector S and $\mathrm{Tr}\,\Phi = S_0$. Positivity of Φ reads $S_0 > 0$, $S_0^2 - S_1^2 - S_2^2 - S_3^2 \geq 0$ corresponding, respectively, to the pair $\mathrm{Tr}\,\Phi > 0$, $\det \Phi \geq 0$. Thus positive 2×2 matrices (or their Stokes vectors) are in one-to-one correspondence with points of the *positive branch of the solid light cone*. Unit trace (intensity) restriction corresponds to the section of this cone at unity along the 'time' axis, $S_0 = 1$. The resulting three-dimensional unit ball $\mathcal{B}_3 \in \mathcal{R}^3$ is the more familiar Bloch (Poincaré) ball, whose surface or boundary $\mathcal{P} = \mathcal{S}^2$ representing pure states (of unit intensity) is often called the Bloch (Poincaré) sphere. The interior points correspond to mixed (partially polarized) states.

Optical systems which map Stokes vectors *linearly* into Stokes vectors have been of particular interest in polarization optics. Such a linear system is represented by a 4×4 real matrix M, the Mueller matrix [231–235] :

$$M \; : S^{\,\mathrm{in}} \rightarrow S^{\,\mathrm{out}} = M S^{\,\mathrm{in}}. \tag{3.2}$$

It is evident that a (physical) Mueller matrix should necessarily map the positive solid light cone into itself. *It needs to respect an additional subtle restriction*, even in classical optics.

Remark : The Mueller-Stokes formulation of classical polarization optics traditionally assumes plane waves. It would appear, within such a framework, one need not possibly

place on a Mueller matrix any more demand than the requirement that it map Stokes vectors to Stokes vectors. However, the very possibility that the input (classical) light could have its polarization and spatial degree of freedoms intertwined in an inseparable manner, leads to the additional requirement that the Mueller matrix acting 'locally' on the polarization indices alone map such an entangled (classical) beam into a physical beam. Interestingly, it is only recently that such a requirement has been pointed out [234, 235], leading to a full characterization of Mueller matrices in classical polarization optics. ■

To see the connection between Mueller matrices and two-qubit states unfold naturally, use a single index rather than a pair of indices to label the computational basis two-qubit states $\{|jk\rangle\}$ in the familiar manner: $(00, 01, 10, 11) = (0, 1, 2, 3)$. Now note that a two-qubit density operator $\hat{\rho}_{AB}$ can be expressed in *two distinct ways*:

$$\begin{aligned} \hat{\rho}_{AB} &= \sum_{j,k=0}^{3} \rho_{jk} |j\rangle\langle k| \\ &= \frac{1}{4} \sum_{a,b=0}^{3} M_{ab}\, \sigma_a \otimes \sigma_b^*, \end{aligned} \tag{3.3}$$

the second expression simply arising from the fact that the sixteen hermitian matrices $\{\sigma_a \otimes \sigma_b^*\}$ form a complete orthonormal set of 4×4 matrices. Hermiticity of operator $\hat{\rho}_{AB}$ is equivalent to reality of the matrix $M = ((M_{ab}))$, but the same hermiticity is equivalent to $\rho = ((\rho_{jk}))$ being a hermitian matrix.

Remark: It is clear from the defining equation (3.3) that the numerical entries of the two matrices ρ, M thus associated with a given two-qubit state $\hat{\rho}_{AB}$ be related in an invertible linear manner. This linear relationship has been in use in polarization optics for a long time [231, 233, 234] and, for convenience, it is reproduced in explicit form in the Appendix. ■

Given a bipartite state $\hat{\rho}_{AB}$, the reduced density operators $\hat{\rho}_A$, $\hat{\rho}_B$ of the subsystems are

readily computed from the associated M :

$$\hat{\rho}_A = \mathrm{Tr}[\hat{\rho}_{AB}] = \frac{1}{2}\sum_{a=0}^{3} M_{a0}\,\sigma_a,$$
$$\hat{\rho}_B = \mathrm{Tr}[\hat{\rho}_{AB}] = \frac{1}{2}\sum_{b=0}^{3} M_{0b}\,\sigma_b^*. \tag{3.4}$$

That is, the leading column and leading row of M are precisely the Stokes vectors of reduced states $\hat{\rho}_A$, $\hat{\rho}_B$ respectively.

It is clear that a generic POVM element is of the form $\Pi_j = \frac{1}{2}\sum_{k=0}^{3} S_k\sigma_k^*$. We shall call S the Stokes vector of the POVM element Π_j. Occasionally one finds it convenient to write it in the form $S = (S_0, \mathbf{S})^T$ with the 'spatial' 3-vector part highlighted. The Stokes vector corresponding to a rank-one element has components that satisfy the relation $S_1^2 + S_2^2 + S_3^2 = S_0^2$. Obviously, rank-one elements are light-like and rank-two elements are strictly time-like. One recalls that similar considerations apply to the density operator of a qubit as well.

The (unnormalised) state operator post measurement (measurement element Π_j) evaluates to

$$\begin{aligned}
\rho^A_{\pi_j} &= \mathrm{Tr}_B[\hat{\rho}_{AB}\,\Pi_j] \\
&= \frac{1}{8}\mathrm{Tr}_B\left[\left(\sum_{a,b=0}^{3} M_{ab}\,\sigma_a\otimes\sigma_b^*\right)\left(\sum_{k=0}^{3} S_k\sigma_k^*\right)\right] \\
&= \frac{1}{8}\sum_{a,b=0}^{3}\sum_{k=0}^{3} M_{ab}\,S_k\,\sigma_a\mathrm{Tr}(\sigma_b^*\sigma_k^*) \\
&= \frac{1}{4}\sum_{a=0}^{3} S_a^{'}\sigma_a,
\end{aligned} \tag{3.5}$$

where we used $\mathrm{Tr}(\sigma_b^*\sigma_k^*) = 2\delta_{bk}$ in the last step.

Remark : It may be noted, for clarity, that we use Stokes vectors to represent both mea-

surement elements and states. For instance, Stokes vector S in Eq. (3.5) stands for a measurement element Π_j on the B-side, whereas $S^{'}$ stands for (unnormalised) state of subsystem A. ■

The Stokes vector of the resultant state in Eq. (3.5) is thus given by $S_a^{'} = \sum_{k=0}^{3} M_{ak} S_k$, which may be written in the suggestive form

$$S^{\text{out}} = M S^{\text{in}}. \tag{3.6}$$

Comparison with (3.2) prompts one to call M the *Mueller matrix associated with two-qubit state* $\hat{\rho}_{AB}$. We repeat that the conditional state $\rho^A_{\pi_j}$ need not have unit trace and so needs to be normalised when computing entropy post measurement. To this end, we write $\rho^A_{\pi_j} = p_j \hat{\rho}_{\pi_j}$, where

$$p_j = \frac{S_0^{\text{out}}}{2}, \;\; \hat{\rho}_{\pi_j} = \frac{1}{2}(\mathbb{1} + (S_0^{\text{out}})^{-1}\, \mathbf{S}^{\text{out}}.\boldsymbol{\sigma}). \tag{3.7}$$

It is sometimes convenient to write the Mueller matrix M associated with a given state $\hat{\rho}_{AB}$ in the block form

$$M = \begin{pmatrix} 1 & \boldsymbol{\xi}^T \\ \boldsymbol{\lambda} & \Omega \end{pmatrix}, \;\; \boldsymbol{\lambda}, \boldsymbol{\xi} \in \mathcal{R}^3.$$

Then the input-output relation (3.6) reads

$$S_0^{\text{out}} = S_0^{\text{in}} + \boldsymbol{\xi} \cdot \mathbf{S}^{\text{in}}, \quad \mathbf{S}^{\text{out}} = S_0^{\text{in}}\, \boldsymbol{\lambda} + \Omega\, \mathbf{S}^{\text{in}}, \tag{3.8}$$

showing in particular that the probability of the conditional state S^{out} on the A-side depends on the POVM element precisely through $1 + \boldsymbol{\xi} \cdot \mathbf{S}^{\text{in}}$.

Remark: The linear relationship between two-qubit density operators ρ (states) and

Mueller matrices (single qubit maps) we have developed in this Section can be usefully viewed as an instance of the Choi-Jamiokowski isomorphism. ■

Remark: We have chosen measurement to be on the B qubit. Had we instead chosen to compute correlations by performing measurements on subsystem A then, by similar considerations as detailed above (3.5), we would have found M^T playing the role of the Mueller matrix M. ■

3.3 X-states and their Mueller matrices

X-states are states whose density matrix ρ has non-vanishing entries only along the diagonal and the anti-diagonal. That is, the numerical matrix ρ has the 'shape' of X. A general X-state can thus be written, to begin with, as

$$\rho_X = \begin{pmatrix} \rho_{00} & 0 & 0 & \rho_{03}e^{i\phi_2} \\ 0 & \rho_{11} & \rho_{12}e^{i\phi_1} & 0 \\ 0 & \rho_{12}e^{-i\phi_1} & \rho_{22} & 0 \\ \rho_{03}e^{-i\phi_2} & 0 & 0 & \rho_{33} \end{pmatrix}, \tag{3.9}$$

where the ρ_{ij}'s are all real nonnegative. One can get rid of the phases (of the off-diagonal elements) by a suitable local unitary transformation $U_A \otimes U_B$. This is not only possible, but *also desirable* because the quantities of interest, namely mutual information, quantum discord and classical correlation, are all invariant under local unitary transformations. Since it is unlikely to be profitable to carry around a baggage of irrelevant parameters, we shall indeed remove ϕ_1, ϕ_2 by taking ρ_X to its canonical form ρ_X^{can}. We have

$$\rho_X \to \rho_X^{\text{can}} = U_A \otimes U_B \rho_X U_A^\dagger \otimes U_B^\dagger, \tag{3.10}$$

where

$$\rho_X^{\text{can}} = \begin{pmatrix} \rho_{00} & 0 & 0 & \rho_{03} \\ 0 & \rho_{11} & \rho_{12} & 0 \\ 0 & \rho_{12} & \rho_{22} & 0 \\ \rho_{03} & 0 & 0 & \rho_{33} \end{pmatrix};$$

$$U_A = \text{diag}(e^{-i(2\phi_1+\phi_2)/4}, e^{i\phi_2/4}),$$

$$U_B = \text{diag}(e^{i(2\phi_1-\phi_2)/4}, e^{i\phi_2/4}). \tag{3.11}$$

Remark : We wish to clarify that X-states thus constitute, in the canonical form, a (real) 5-parameter family ($\rho_{00}+\rho_{11}+\rho_{22}+\rho_{33} = m_{00} = 1$); it can be lifted, using local unitaries U_A, $U_B \in SU(2)$ which have three parameters each, to a 11-parameter subset in the 15-parameter state space (or generalized Bloch sphere) of two-qubit states : they are all local unitary equivalent though they may no more have a 'shape' X.

With this canonical form, it is clear that the Mueller matrix for the generic X-state ρ_X^{can} has the form

$$M = \begin{pmatrix} 1 & 0 & 0 & m_{03} \\ 0 & m_{11} & 0 & 0 \\ 0 & 0 & m_{22} & 0 \\ m_{30} & 0 & 0 & m_{33} \end{pmatrix}, \tag{3.12}$$

where

$$m_{11} = 2(\rho_{03}+\rho_{12}), \;\; m_{22} = 2(\rho_{03}-\rho_{12}),$$

$$m_{03} = \rho_{00}+\rho_{22}-(\rho_{11}+\rho_{33}),$$

$$m_{33} = \rho_{00}+\rho_{33}-(\rho_{11}+\rho_{22}),$$

$$m_{30} = \rho_{00}+\rho_{11}-(\rho_{22}+\rho_{33}), \tag{3.13}$$

as can be read off from the defining equation (3.3) or Eq. (3.92) in the Appendix. We note that the Mueller matrix of an X-state has a 'sub-X' form : the only nonvanishing off-diagonal entries are m_{03} and m_{30} ($m_{12} = 0 = m_{21}$). In our computation later we will sometimes need the inverse relations

$$\begin{aligned}
\rho_{00} &= \frac{1}{4}(m_{00} + m_{03} + m_{30} + m_{33}),\\
\rho_{11} &= \frac{1}{4}(m_{00} - m_{03} + m_{30} - m_{33}),\\
\rho_{22} &= \frac{1}{4}(m_{00} + m_{03} - m_{30} - m_{33}),\\
\rho_{33} &= \frac{1}{4}(m_{00} - m_{03} - m_{30} + m_{33}),\\
\rho_{03} &= \frac{1}{4}(m_{11} + m_{22}),\ \ \rho_{12} = \frac{1}{4}(m_{11} - m_{22}).
\end{aligned} \tag{3.14}$$

The positivity properties of $\rho_X^{\rm can}$, namely $\rho_{00}\rho_{33} \geq \rho_{03}^2$, $\rho_{11}\rho_{22} \geq \rho_{12}^2$ transcribes to the following conditions on the entries of its Mueller matrix :

$$(1 + m_{33})^2 - (m_{30} + m_{03})^2 \geq (m_{11} + m_{22})^2 \tag{3.15}$$

$$(1 - m_{33})^2 - (m_{30} - m_{03})^2 \geq (m_{11} - m_{22})^2. \tag{3.16}$$

Remark : As noted earlier the requirements (3.15), (3.16) on classical optical Mueller matrix (3.12) was noted for the first time in Refs. [234, 235]. These correspond to complete positivity of M considered as a positive map (map which images the solid light cone into itself), and turns out to be equivalent to positivity of the corresponding two-qubit density operator. ■

By virtue of the direct-sum block structure of X-state density matrix, one can readily write down its (real) eigenvectors. We choose the following order

$$\begin{aligned}
|\psi_0\rangle &= c_\alpha|00\rangle + s_\alpha|11\rangle,\ \ |\psi_1\rangle = c_\beta|01\rangle + s_\beta|10\rangle,\\
|\psi_2\rangle &= -s_\beta|01\rangle + c_\beta|10\rangle,\ |\psi_3\rangle = -s_\alpha|00\rangle + c_\alpha|11\rangle,
\end{aligned} \tag{3.17}$$

where $c_\alpha,\ s_\alpha$ denote respectively $\cos\alpha$ and $\sin\alpha$. And (dropping the superscript 'can') we have the spectral resolution

$$\hat{\rho}_X = \sum_{j=0}^{3} \lambda_j |\psi_j\rangle\langle\psi_j|, \tag{3.18}$$

$$\begin{aligned}
c_\alpha &= \sqrt{\frac{1+\nu_1}{2}},\ c_\beta = \sqrt{\frac{1+\nu_2}{2}}, \\
\nu_1 &= \frac{\rho_{00}-\rho_{33}}{\sqrt{4\rho_{03}^2+(\rho_{00}-\rho_{33})^2}} = \frac{m_{30}+m_{03}}{\sqrt{(m_{11}+m_{22})^2+(m_{30}+m_{03})^2}}, \\
\nu_2 &= \frac{\rho_{11}-\rho_{22}}{\sqrt{4\rho_{12}^2+(\rho_{11}-\rho_{22})^2}} = \frac{m_{30}-m_{03}}{\sqrt{(m_{11}-m_{22})^2+(m_{30}-m_{03})^2}}; \\
\lambda_{0\,\text{or}\,3} &= \frac{\rho_{00}+\rho_{33}}{2} \pm \frac{\sqrt{(\rho_{00}-\rho_{33})^2+4\rho_{03}^2}}{2} \\
&= \frac{1+m_{33}}{4} \pm \frac{\sqrt{(m_{11}+m_{22})^2+(m_{30}+m_{03})^2}}{4}, \\
\lambda_{1\,\text{or}\,2} &= \frac{\rho_{11}+\rho_{22}}{2} \pm \frac{\sqrt{(\rho_{11}-\rho_{22})^2+4\rho_{12}^2}}{2} \\
&= \frac{1-m_{33}}{4} \pm \frac{\sqrt{(m_{11}-m_{22})^2+(m_{30}-m_{03})^2}}{4}.
\end{aligned} \tag{3.19}$$

While computation of $S^A_{\min}$ will have to wait for a detailed consideration of the manifold of conditional states of $\hat{\rho}_{AB}$, the other entropic quantities can be evaluated right away. Given a qubit state specified by Stokes vector $(1, \mathbf{S})^T$, it is clear that its von Neumann entropy equals

$$S_2(r) = -\left[\frac{1+r}{2}\right] \ell og_2\left[\frac{1+r}{2}\right] - \left[\frac{1-r}{2}\right] \ell og_2\left[\frac{1-r}{2}\right], \tag{3.20}$$

where r is the norm of the three vector $\mathbf{S}$, or the distance of $\mathbf{S}$ from the origin of the Bloch

ball. Thus from Eq. (3.4) we have

$$S(\hat{\rho}_A) = S_2(|m_{30}|),\ S(\hat{\rho}_B) = S_2(|m_{03}|),$$
$$S(\hat{\rho}_{AB}) \equiv S(\{\lambda_j\}) = \sum_{j=0}^{3} -\lambda_j \ell og_2(\lambda_j), \tag{3.21}$$

where $\lambda_j,\ j = 0,1,2,3$ are the eigenvalues of the bipartite state $\hat{\rho}_{AB}$ given in Eq. (3.19). The mutual information thus assumes the value

$$I(\hat{\rho}_{AB}) = S_2(|m_{30}|) + S_2(|m_{03}|) - S(\{\lambda_j\}). \tag{3.22}$$

3.4 Correlation ellipsoid : Manifold of conditional states

We have seen that the state of subsystem A resulting from measurement of any POVM element on the B-side of $\hat{\rho}_{AB}$ is the Stokes vector resulting from the action of the associated Mueller matrix on the Stokes vector of the POVM element. In the case of rank-one measurement elements, the 'input' Stokes vectors correspond to points on the (surface $\mathcal{S}^2 = \mathcal{P}$ of the) Bloch ball. Denoting the POVM elements as $S^{\text{in}} = (1, x, y, z)^T$, $x^2 + y^2 + z^2 = 1$, we ask for the collection of corresponding normalized or conditional states. By Eq. (3.6) we have

$$S^{\text{out}} = MS^{\text{in}} = \begin{pmatrix} 1 + m_{03}z \\ m_{11}\,x \\ m_{22}\,y \\ m_{30} + m_{33}\,z \end{pmatrix} \rightarrow \begin{pmatrix} 1 \\ \frac{m_{11}\,x}{1+m_{03}z} \\ \frac{m_{22}\,y}{1+m_{03}z} \\ \frac{m_{30}+m_{33}\,z}{1+m_{03}z} \end{pmatrix}, \tag{3.23}$$

It is clear that, for $S_0^{\text{in}} = 1$, $S_0^{\text{out}} \neq 1$ whenever $m_{03} \neq 0$ and the input is *not* in the x-y plane of the Poincaré sphere. It can be shown that the sphere $x^2 + y^2 + z^2 = 1$ at the 'input' is

mapped to the ellipsoid

$$\frac{x^2}{a_x^2} + \frac{y^2}{a_y^2} + \frac{(z - z_c)^2}{a_z^2} = 1 \tag{3.24}$$

of normalized states at the output, the parameters of the ellipsoid being fully determined by the entries of M:

$$\begin{aligned} a_x &= \frac{|m_{11}|}{\sqrt{1 - m_{03}^2}}, \quad a_y = \frac{|m_{22}|}{\sqrt{1 - m_{03}^2}}, \\ a_z &= \frac{|m_{33} - m_{03}m_{30}|}{1 - m_{03}^2}, \quad z_c = \frac{m_{30} - m_{03}m_{33}}{1 - m_{03}^2}. \end{aligned} \tag{3.25}$$

Remark: This ellipsoid of all possible (normalized) conditional states associated with a two-qubit state is something known as a steering ellipsoid [223, 237–239]. It degenerates into a single point if and only if the state is a product state. It captures in a geometric manner correlations in the two-qubit state under consideration, and correlation is the object of focus of the present work. For those reasons, we prefer to call it the *correlation ellipsoid* associated with the given two-qubit state. While measurement elements Π_j are mapped to points of the ellipsoid, measurement elements $a\Pi_j$ for all $a > 0$ are mapped to one and the same point of the correlation ellipsoid. Thus, in the general case, each point of the ellipsoid corresponds to a 'ray' of measurement elements. In the degenerate case, several rays map to the same point. ■

The x-z section of the correlation ellipsoid is pictorially depicted in Fig. 3.1. It is clear that the geometry of the ellipsoid is determined by the four parameters a_x, a_y, a_z, z_c and z_c could be assumed nonnegative without loss of generality. The fifth parameter m_{30} specifying the z-coordinate of the image I of the maximally mixed state on the B side is not part of this geometry.

Having thus considered the passage from a two-qubit X-state to its correlation ellipsoid, we may raise the converse issue of going from the correlation ellipsoid to the associated

X-state. To do this, however, we need the parameter $z_I = m_{30}$ as an input in addition to the ellipsoid itself. Further, change of the signature of m_{22} does not affect the ellipsoid in any manner, but changes the states and correspondingly the signature of det$M$. Thus, the signature of det$M$ needs to be recorded as an additional binary parameter. It can be easily seen that the nonnegative a_x, a_y, a_z, z_c along with z_I and sgn (det$M$) fully reconstruct the X-state in its canonical form (3.12). Using local unitary freedom we can render m_{11}, $m_{33} - m_{03}m_{30}$ and z_c nonnegative so that sgn(m_{22}) = sgn (det$M$); $z_I = m_{30}$ can assume either signature. It turns out to be convenient to denote by Ω^+ the collection of all Mueller matrices with det$M \geq 0$ and by Ω^- those with det$M \leq 0$. The intersection corresponds to Mueller matrices for which det$M = 0$, a measure zero set. Further, in our analysis to follow we assume, without loss of generality

$$a_x \geq a_y. \tag{3.26}$$

Remark: Every two-qubit state has associated with it a unique correlation ellipsoid of (normalized) conditional states. An ellipsoid centered at the origin needs six parameters for its description: three for the sizes of the principal axes and three for the orientation of the ellipsoid as a rigid body. For a generic state, the centre C can be shifted from the origin to vectorial location $\vec{r}_c$, thus accounting for three parameters, and I can be located at $\vec{r}_I$ anywhere inside the ellipsoid, thus accounting for another three. The three-parameter local *unitary* transformations on the B-side, having no effect whatsoever on the geometry of the ellipsoid, (but determines which points of the input Poincaré sphere go to which points on the surface of the ellipsoid), accounts for the final three parameters, adding to a total of 15. For X-states the shift of C from the origin *needs to be* along one of the principal directions and I is *constrained to be located on this very principal axis*. In other words, $\vec{r}_c$ and $\vec{r}_I$ become one-dimensional rather than three-dimensional variables rendering X-states a 11-parameter subfamily of the 15-parameter state space. *Thus X-states are distinguished by the fact that C,* I, *and the origin are collinear with one of the*

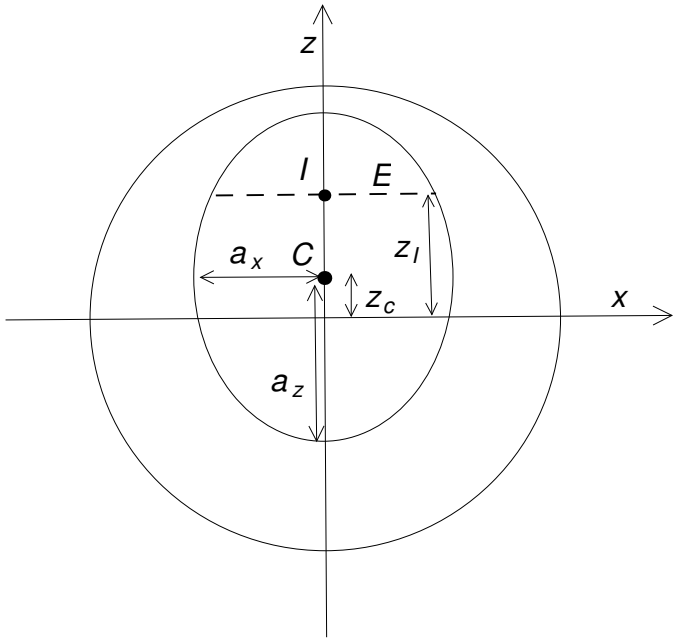

Figure 3.1: Showing the x-z cross-section of the correlation ellipsoid associated with a general X-state. The point I is the image of input state as identity, C the center of the ellipsoid, and E the image of the equatorial plane of the input Bloch sphere.

principal axes of the ellipsoid. This geometric rendering pays no special respect to the shape X, but is manifestly invariant under local unitaries as against the characterization in terms of 'shape' X of the matrix ρ_{AB} in the computation basis. *The latter characterization is not even invariant under local unitaries!* ■

3.5 Optimal measurement

In this Section we take up the central part of the present work which is to develop a provably optimal scheme for computation of the quantum discord for any X-state of a two-qubit system. Our treatment is *both comprehensive and self-contained and, moreover, it is geometric in flavour*. We begin by exploiting symmetry to show, without loss of generality, that the problem itself is one of *optimization in just a single variable*. The analysis is entirely based on the output or correlation ellipsoid associated with a two-qubit

state $\hat{\rho}_{AB}$, and we continue to assume that measurements are carried out on the B-side.

The single-variable function under reference will be seen, on optimization, to divide the manifold of possible correlation ellipsoids into two subfamilies. For one subfamily the optimal measurement or POVM will be shown to be a von Neumann measurement along either x or z, *independent of the location (inside the ellipsoid) of* I, *the image of the maximally mixed input*. For the other subfamily, the optimal POVM will turn out to be either a von Neumann measurement along x or a three-element POVM, *depending on the actual location of* I *in the ellipsoid*. There exists no X-state for which the optimal measurement requires a four-element POVM, neither does there exist an X-state for which the optimal POVM is von Neumann neither along x nor z.

For the special case of the centre C of the ellipsoid coinciding with the origin $z = 0$ of the Poincaré sphere ($z_c = 0$), it will be shown that the optimal measurement is always a von Neumann measurement along x or z, *irrespective of the location of* z_I *in the ellipsoid*. While this result may look analogous to the simple case of Bell mixtures earlier treated by Luo [219], it should be borne in mind that these centred X-states form a much larger family than the family of Bell mixtures, for in the Luo scenario I *coincides with C and hence with the origin*, but we place no such restriction of coincidence. Stated differently, in our case a_x, a_y, a_z and z_I are independent variables.

As we now turn to the analysis itself it is useful to record this : the popular result that the optimal POVM requires no more than four elements plays *a priori* no particular role of help in our analysis; it is for this reason that we shall have no occasion in our analysis to appeal to this important theorem [240, 241].

Proposition : The optimal POVM needs to comprise rank-one elements.

Proof : This fact is nearly obvious, and equally obvious is its proof. Suppose ω_j is a rank-two element of an optimal POVM and $\hat{\rho}_j^A$ the associated conditional state of subsystem A. Write ω_j as a positive sum of rank-one elements ω_{j1}, ω_{j2} and let $\hat{\rho}_{j1}^A$, $\hat{\rho}_{j2}^A$

be the conditional states corresponding respectively to ω_{j1}, ω_{j2}. It is then clear that $\hat{\rho}_j = \lambda\hat{\rho}^A_{j1} + (1-\lambda)\hat{\rho}^A_{j2}$, for some $0 < \lambda < 1$. Concavity of the entropy function immediately implies $S(\hat{\rho}^A_j) > \lambda S(\hat{\rho}^A_{j1}) + (1-\lambda)S(\hat{\rho}^A_{j2})$, in turn implying through (1.57) that the POVM under consideration could not have been optimal. It is clear from the nature of the proof that this fact applies to all Hilbert space dimensions, and not just $d = 2$. ■

Remark: Since a rank-one POVM element $|v\rangle\langle v|$ is just a point $\mathbf{S}$ on (the surface of) the Bloch (Poincaré) sphere $\mathcal{P}$, a four element rank-one POVM is a quadruple of points $\mathbf{S^{(j)}}$ on $\mathcal{P}$, with associated probabilities p_j. The POVM condition $\sum_j p_j|v_j\rangle\langle v_j| = \mathbb{1}$ demands that we have to solve the pair

$$\begin{aligned} p_1 + p_3 + p_3 + p_4 &= 2, \\ \sum_j p_j \mathbf{S^{(j)}} &= 0. \end{aligned} \tag{3.27}$$

Once four points $\mathbf{S^{(j)}}$ on $\mathcal{P}$ are chosen, the 'probabilities' $\{p_j\}$ are *not independent*. To see this, consider the tetrahedron for which $\mathbf{S^{(j)}}$ are the vertices. If this tetrahedron does not contain the origin, then $\sum_j p_j\mathbf{S^{(j)}} = 0$ has no solution with nonnegative $\{p_j\}$. If it contains the origin, then there exits a solution and the solution is 'essentially' unique by Caratheodory theorem.

The condition $\sum_j p_j = 2$ comes into play in the following manner. Suppose we have a solution to $\sum_j p_j \mathbf{S^{(j)}} = 0$. It is clear that $p_j \to p_j^{'} = ap_j$, $j = 1, 2, 3, 4$, with no change in $\mathbf{S^{(j)}}$'s, will also be a solution for any (j-independent) $a > 0$. It is this freedom in choosing the scale parameter a that gets frozen by the condition $\sum_j p_j = 2$, rendering the association between tetrahedra and solutions of the pair (3.27) unique.

We thus arrive at a geometric understanding of the manifold of all (rank-one) four-element POVM's, even though we would need such POVM's only when we go beyond X-states. This is precisely the manifold of all tetrahedra with vertices on $\mathcal{P}$, and containing the

centre in the interior of $\mathcal{P}$. We are not considering four-element POVM's whose $\mathbf{S}^{(j)}$ are coplanar with the origin of $\mathcal{P}$, because they are of no use as optimal measurements. It is clear that three element rank-one POVM's are similarly characterized, again by the Caratheodory theorem, by triplets of points on $\mathcal{P}$ coplanar with the origin of $\mathcal{P}$, with the requirement that the triangle generated by the triplet contains the origin *in the interior*. Further, it is trivially seen in this manner that 2-element rank-one POVM's are von Neumann measurements determined by pairs of antipodal $\mathbf{S}^{(j)}$'s on $\mathcal{P}$, i.e., by 'diameters' of $\mathcal{P}$. ■

The correlation ellipsoid of an X-state (as a subset of the Poincaré sphere) has a $\mathcal{Z}_2 \times \mathcal{Z}_2$ symmetry generated by reflections respectively about the x-z and y-z planes. We shall now use the product of these two reflections—a π-rotation or inversion about the z-axis—to simplify, without loss of generality, our problem of optimization.

Proposition : All elements of the optimal POVM have to necessarily correspond to Stokes vectors of the form $S_0(1,\, \sin\theta,\, 0,\, \cos\theta)^T$.

Proof: Suppose $\mathcal{N} = \{\omega_1, \omega_2, \cdots, \omega_k\}$ is an optimal POVM of rank-one elements (we are placing no restriction on the cardinality k of $\mathcal{N}$, but rather allow it to unfold naturally from the analysis to follow). And let $\{\hat{\rho}_1^A, \hat{\rho}_2^A, \cdots, \hat{\rho}_k^A\}$ be the corresponding conditional states, these being points on the boundary of the correlation ellipsoid. Let $\tilde{\omega}_j$ and $\tilde{\hat{\rho}}_j^A$ represent, respectively, the images of ω_j, $\hat{\rho}_j^A$ under π-rotation about the z-axis (of the input Poincaré sphere and of the correlation ellipsoid). It follows from symmetry that $\widetilde{\mathcal{N}} = \{\tilde{\omega}_1, \tilde{\omega}_2, \cdots, \tilde{\omega}_k\}$ too is an optimal POVM. And so is also $\mathcal{N} \overline{\bigcup} \widetilde{\mathcal{N}}$, where we have used the decorated symbol $\overline{\bigcup}$ rather than the set union symbol $\bigcup$ to distinguish from simple union of sets: if $S_0(\mathbb{1} \pm \sigma_3)$ happens to be an element ω_j of $\mathcal{N}$, then $\tilde{\omega}_j = w_j$ for this element, and in that case this ω_j should be 'included' in $\mathcal{N} \overline{\bigcup} \widetilde{\mathcal{N}}$ *not once but twice* (equivalently its 'weight' needs to be doubled). The same consideration holds if $\mathcal{N}$ includes ω_j and $\sigma_3\, \omega_j\, \sigma_3$.

Our supposed to be optimal POVM thus comprises pairs of elements ω_j, $\tilde{\omega}_j$ related by inversion about the z-axis : $\tilde{\omega}_j = \sigma_3 \omega_j \sigma_3$. Let us consider the associated conditional states $\hat{\rho}_j^A$, $\tilde{\hat{\rho}}_j^A$ on the (surface of the) correlation ellipsoid. They have identical z-coordinate z_j. The section of the ellipsoid (parallel to the x-y plane) at $z = z_j$ is an ellipse, with major axis along x (recall that we have assumed, without loss of generality $a_x \geq a_y$), and $\hat{\rho}_j^A$ and $\tilde{\hat{\rho}}_j^A$ are on opposite ends of a line segment through the centre z_j of the ellipse. Let us *assume* that this line segment is not the major axis of the ellipse $z = z_j$. That is, we assume $\hat{\rho}_j^A$, $\tilde{\hat{\rho}}_j^A$ are not in the x-z plane.

Now slide (only) this pair along the ellipse smoothly, keeping them at equal and opposite distance from the z-axis until both reach opposite ends of the major axis of the ellipse, the x-z plane. It is clear that during this process of sliding $\hat{\rho}_j^A$, $\tilde{\hat{\rho}}_j^A$ recede away from the centre of the ellipse and hence away from the centre of the Poincaré sphere itself. As a result $S(\hat{\rho}_j^A)$ decreases, thus improving the value of $S^A_{\min}$ in (1.57). This would have proved that the POVM $\mathcal{N}$ is not optimal, unless our assumption that $\hat{\rho}_j^A$, $\tilde{\hat{\rho}}_j^A$ are not in the x-z plane is false. This completes proof of the proposition. ■

This preparation immediately leads to the following important result which forms the basis for our further analysis.

Theorem 8 *: The problem of computing quantum discord for X-states is a problem of convex optimization on a plane or optimization over a single variable.*

Proof: We have just proved that elements of the optimal POVM come, in view of the $\mathcal{Z}_z \times \mathcal{Z}_2$ symmetry of X-states, in pairs $S_0(1, \pm\sin\theta, 0, \cos\theta)^T$ of Stokes vectors ω_j, $\tilde{\omega}_j$ with $0 \leq \theta \leq \pi$. The corresponding conditional states come in pairs $\hat{\rho}_j^A$, $\tilde{\hat{\rho}}_j^A = 1/2(\mathbb{1} \pm x_j\sigma_1 + z_j\sigma_3)$. The two states of such a pair of conditional states are at the same distance

$$r(z_j) = \sqrt{z_j^2 + a_x^2 - (z_j - z_c)^2 a_x^2/a_z^2} \tag{3.28}$$

from the origin of the Poincaré sphere, and hence they have the same von Neumann

entropy

$$f(z_j) = S_2(r(z_j)),$$
$$S_2(r) = -\frac{1+r}{2}\,\ell og_2\,\frac{1+r}{2} - \frac{1-r}{2}\,\ell og_2\,\frac{1-r}{2}. \tag{3.29}$$

Further, continuing to assume without loss of generality $a_x \geq a_y$, our convex optimization is not over the three-dimensional ellipsoid, but effectively a *planar* problem over the x-z elliptic section of the correlation ellipsoid, and hence the optimal POVM cannot have more that three elements. Thus, the (Stokes vectors of the) optimal POVM elements on the B-side necessarily have the form,

$$\Pi_\theta^{(3)} = \{2p_0(\theta)(1,0,0,1)^T,\ 2p_1(\theta)(1,\pm\sin\theta,0,-\cos\theta)^T\},$$
$$p_0(\theta) = \frac{\cos\theta}{1+\cos\theta},\quad p_1(\theta) = \frac{1}{2(1+\cos\theta)},\ 0 \leq \theta \leq \pi/2. \tag{3.30}$$

The optimization itself is thus over the single variable θ. ■

Remark: It is clear that $\theta = 0$ and $\theta = \pi/2$ correspond respectively to von Neumann measurement along z and x, and no other von Neumann measurement gets included in Π_θ. Every Π_θ in the open interval $0 < \theta < \pi/2$ corresponds to a *genuine* three-element POVM.

The symmetry considerations above do allow also three-element POVM's of the form

$$\widetilde{\Pi}_\theta^{(3)} = \{2p_0(\theta)(1,0,0,-1)^T,\ 2p_1(\theta)(1,\pm\sin\theta,0,\cos\theta)^T\},\quad 0 \leq \theta \leq \pi/2, \tag{3.31}$$

but such POVM's lead to local maximum rather than a minimum for S^A, and hence are of no value to us. ■

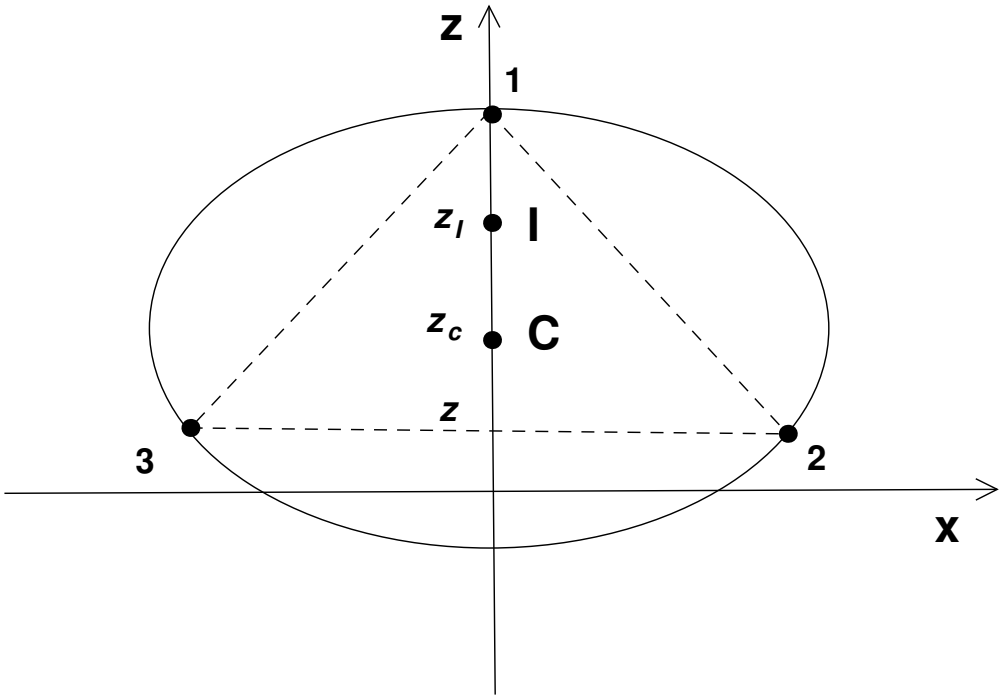

Figure 3.2: Showing the conditional states corresponding to the 3-element measurement scheme of (3.30).

3.6 Computation of $S^A_{\min}$

A schematic diagram of the 3-element POVM $\Pi^{(3)}_\theta$ of Eq. (3.30) is shown in Fig. 3.2. The Bloch vectors of the corresponding conditional states $\hat{\rho}^A_1$, $\hat{\rho}^A_2$, $\hat{\rho}^A_3$ at the output are found to be of the form

$$(0,\ 0,\ z_c + a_z)^T, (x(z),\ 0,\ z)^T,\ (-x(z),\ 0,\ z)^T,$$
$$x(z) = \frac{a_x}{a_z}(a_z^2 - (z - z_c)^2)^{1/2}. \tag{3.32}$$

For these states denoted $1, 2, 3$ in Fig. 3.2 the weights should be chosen to realize as convex sum the state I (the image of the maximally mixed input) whose Bloch vector is $(0, 0, z_I)^T$. The von Neumann measurements along the z or x-axis correspond respectively to $z = z_c - a_z$ or z_I. Using Eqs. (3.28), (3.29), the expression for $S^A(z)$ is thus given by

$$S^A(z) = p_1(z)\, f(z_c + a_z) + p_2(z)\, f(z),$$
$$p_1(z) = \frac{z_I - z}{z_c + a_z - z}, \quad p_2(z) = \frac{z_c + a_z - z_I}{z_c + a_z - z}. \tag{3.33}$$

The minimization of $S^A(z)$ with respect to the single variable z should give $S^A_{\min}$. It may be noted in passing that, for a given I or z_I, the three-element POVM parametrized by z is of no value in the present context for $z > z_I$.

For clarity of presentation, we begin by considering a specific example $(a_z,\, z_c,\, z_I) = (0.58,\, 0.4, 0.6)$. The relevant interval for the variable z in this case is $[z_c - a_z,\, c + a_z] = [-0.18, 0.98]$, and we shall examine the situation as we vary a_x for fixed (a_z, z_c, z_I). The behaviour of $S^A(z)$ for this example is depicted in Fig. 3.3, wherein each curve in the $(z,\, S^A(z))$ plane corresponds to a chosen value of a_x, and the value of a_x increases as we go down Fig. 3.3. For values of $a_x \leq a_x^V(a_z, z_c)$, for some $a_x^V(a_z, z_c)$ to be detailed later, $S^A(z)$ is seen to be a monotone increasing function of z, and so its minimum $S^A_{\min}$ obtains at the 'lower' end point $z = z_c - a_z = -0.18$, hence the optimal POVM corresponds to the vertical projection or von Neumann measurement along the z-axis. The curve marked 2 corresponds to $a_x = a_x^V(a_z, z_c)$ [which equals 0.641441 for our example].

Similarly for values of $a_x \geq a_x^H(a_z, z_c)$, $S^A(z)$ proves to be a monotone decreasing function of z, its minimum therefore obtains at the 'upper' end point which is z_I and not $z_c + a_z$ [recall that the three-element POVM makes no sense for $z > z_I$]; hence the optimal POVM corresponds to horizontal projection or von Neumann measurement along x-axis. It will be shown later that both $a_x^V(a_z, z_c)$, $a_x^H(a_z, z_c)$ do indeed depend only on a_z, z_c and not on z_I. Both are therefore properties of the ellipsoid : all states with one and the same ellipsoid will share the same $a_x^V(a_z, z_c)$, $a_x^H(a_z, z_c)$.

Thus, it is the region $a_x^V(a_z, z_c) < a_x < a_x^H(a_z, z_c)$ of values of a_x that needs a more careful analysis, for it is only in this region that the optimal measurement could possibly correspond to a three-element POVM. Clearly, this region in the space of correlation ellipsoids is distinguished by the fact that $S^A(z)$ has a minimum at some value $z = z_0$ in the open

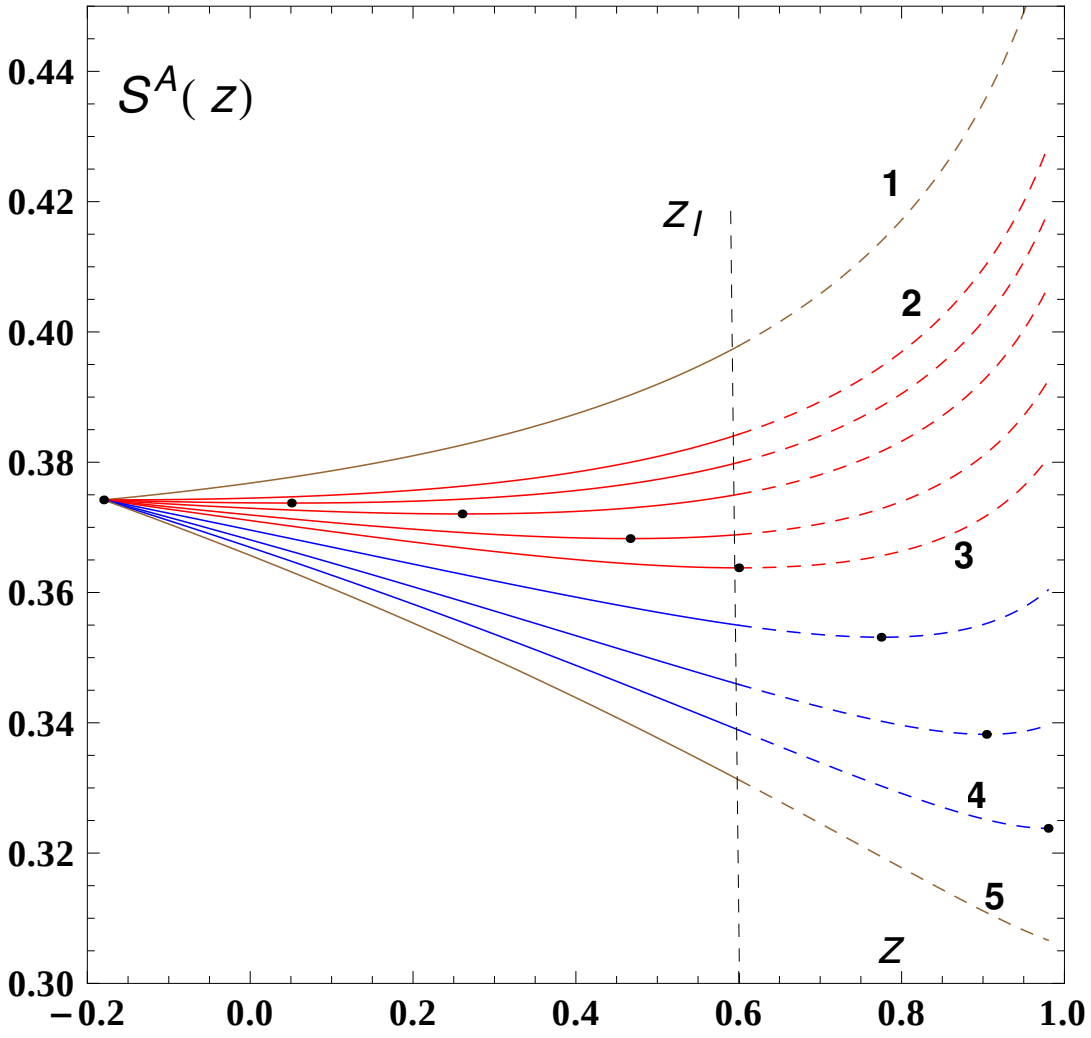

Figure 3.3: Showing $S^A(z)$ for various values of a_x labelled in increasing order. The line marked z_I denotes $z = z_I$. A three-element POVM scheme results for values of $a_x \in (a_x^V(a_z, z_c), a_x^H(a_z, z_c))$ [the curves (2) and (4)]. For values of $a_x \leq a^V(a_z, z_c)$ [example of curve (1)], the von Neumann projection along the z-axis is the optimal and for values of $a_x \geq a^H(a_z, z_c)$ [example of curve (5)], the von Neumann projection along the x-axis is the optimal. The optimal $z = z_0$ is obtained by minimizing $S^A(z)$ (marked with a dot). $S^A(z)$ for $z > z_I$ is not meaningful and this region of the curves is shown with dashed lines. In this example $(a_z, z_c) = (0.58, 0.4, 0.6)$. For $z_I = 0.6$, a three-element POVM results for (red) curves between (2) and (3).

interval $(z_c - a_z,\, z_c + a_z)$. For $a_x = a_x^V(a_z, z_c)$ this minimum occurs at $z_0 = z_c - a_z$, moves with increasing values of a_x gradually towards $z_c + a_z$, and reaches $z_c + a_z$ itself as a_x reaches $a_x^H(a_z, z_c)$.

Not only this qualitative behaviour, but also the exact value of $z_0(a_z, z_c, a_x)$ is independent of z_I, as long as $z_c \neq 0$. Let us evaluate $z_0(a_z, z_c, a_x)$ by looking for the zero-crossing of the derivative function $dS^A(z)/dz$ depicted in Fig. 3.4. We have

$$\begin{aligned}
\frac{d\,S^A(z)}{dz} &= (z_c + a_z - z_I)\, G(a_z, a_x, z_c; z), \\
G(a_z, a_x, z_c; z) &= \frac{1}{(z_c + a_z - z)^2} \Big([(z_c + a_z - z)(a_x^2(z - z_c)/a_z^2 - z) X(z)] \\
&\qquad\qquad - [f(z_c + a_z) - f(z)] \Big), \\
X(z) &= \frac{1}{2r(z)} \ell og_2 \left[\frac{1 + r(z)}{1 - r(z)} \right],
\end{aligned} \tag{3.34}$$

and we need to look for z_0 that solves $G(a_z, a_x, z_c; z_0) = 0$. The reader may note that z_I *does not enter* the function $G(a_z, a_x, z_c; z_0)$ defined in Eq. (3.34), showing that z_0 is indeed independent of z_I as claimed earlier : *z_0 is a property of the correlation ellipsoid; all states with the same correlation ellipsoid have the same z_0*.

Let us focus on the two curves $a_x^V(a_z, z_c)$, $a_x^H(a_z, z_c)$ introduced earlier and defined through

$$\begin{aligned}
a_x^V(a_z, z_c) &: \; G(a_z, a_x^V, z_c; z_c - a_z) = 0, \\
a_x^H(a_z, z_c) &: \; G(a_z, a_x^H, z_c; z_c + a_z) = 0.
\end{aligned} \tag{3.35}$$

The curve $a_x^V(a_z, z_c)$ characterizes, for a given (a_z, z_c), the value of a_x for which the first derivative of $S^A(z)$ vanishes at $z = z_c - a_z$ (i.e., $z_0 = z_c - a_z$), so that the vertical von Neumann projection is the optimal POVM for all $a_x \leq a_x^V(a_z, z_c)$. Similarly, the curve $a_x^H(a_z, z_c)$ captures the value of a_x for which the first derivative of $S^A(z)$ vanishes at $z =$

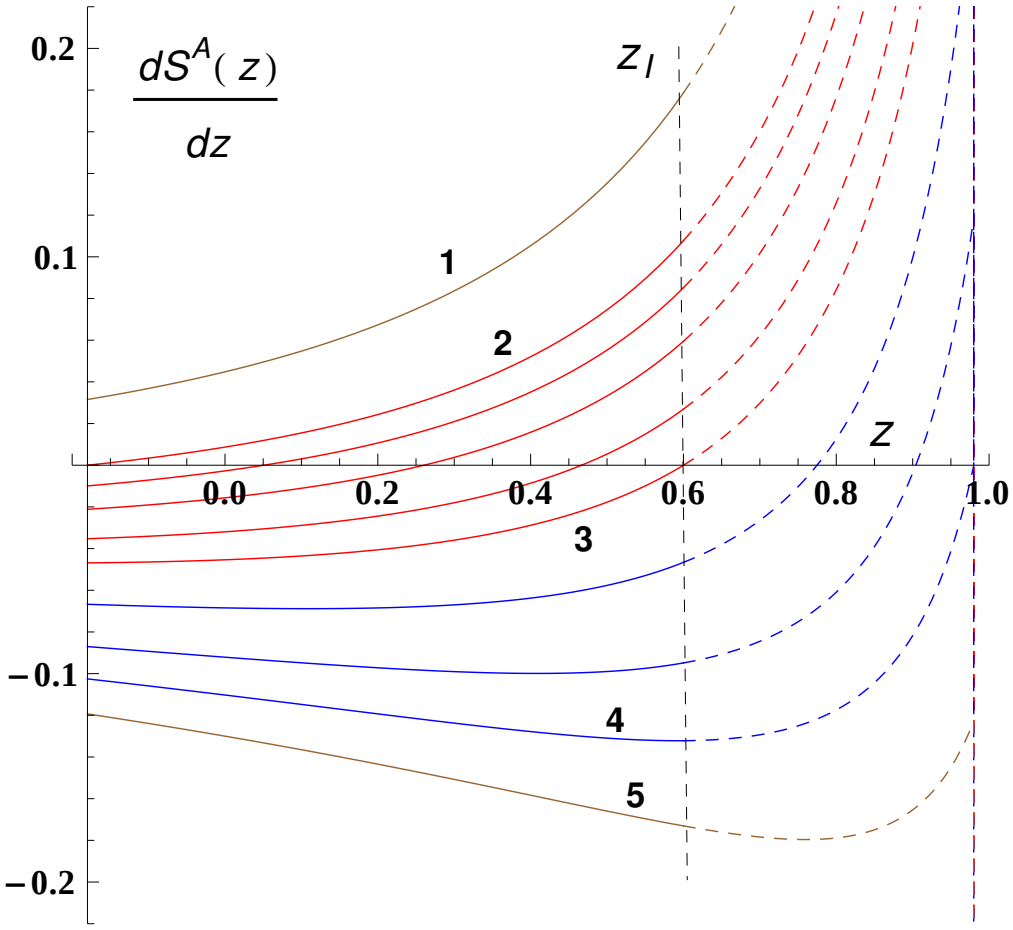

Figure 3.4: Showing $dS^A(z)/dz$ for various values of a_x labelled in increasing order. A root exits for values of $a_x \in (a_x^V(a_z, z_c), a_x^H(a_z, z_c))$ [between curves (2) and (4)]. For values of $a_x \leq a^V(a_z, z_c)$ and $a_x \geq a^H(a_z, z_c)$, there is no z_0 [examples are curves (1) and (5)].

$z_c + a_z$. Solving for the two curves in terms of a_z and z_c we obtain, after some algebra,

$$
\begin{aligned}
a_x^V(a_z, z_c) &= \sqrt{\frac{f(|z_c - a_z|) - f(z_c + a_z)}{2X(|z_c - a_z|)}} - a_z(z_c - a_z), \\
a_x^H(a_z, z_c) &= \frac{(z_c + a_z)}{2[Y(z_c + a_z) - X(z_c + a_z)]} \\
&\qquad \times \left[(z_c - a_z)X(z_c + a_z) + 2a_z Y(z_c + a_z) - \sqrt{w}\right], \\
Y(z) &= \frac{1}{[\ell n\, 2\,](1 - r(z)^2)}, \\
w &= X(z_c + a_z)[(z_c - a_z)^2 X(z_c + a_z) + 4a_z z_c Y(z_c + a_z)].
\end{aligned} \tag{3.36}
$$

These curves are marked (1) and (2) respectively in Fig. 3.5. Two aspects are of particular importance :

(i) $a_x^H(a_z, z_c) \geq a_x^V(a_z, z_c)$, the inequality saturating if and only if $z_c = 0$. In particular these two curves never meet, the appearance in Fig. 3.5 notwithstanding. It is to emphasize this fact that an inset has been added to this figure. The straight line $a_x = a_z$, marked (3) in Fig. 3.5, shows that $a_x^V(a_z, z_c) \geq a_z$, the inequality saturating if and only if $z_c = 0$.

(ii) It is only in the range $a_x^V(a_z, z_c) < a_x < a_x^H(a_z, z_c)$ that we get a solution z_0

$$
G(a_z, a_x, z_c; z_0) = 0, \quad z_c - a_z < z_0 < z_c + a_z \tag{3.37}
$$

corresponding to a *potential* three-element optimal POVM for *some* X-state corresponding to the ellipsoid under consideration; and, clearly, the optimal measurement for the state will *actually* correspond to a three-element POVM only if

$$
z_I > z_0. \tag{3.38}
$$

If $z_I \leq z_0$, the optimal measurement corresponds to a von Neumann projection along the

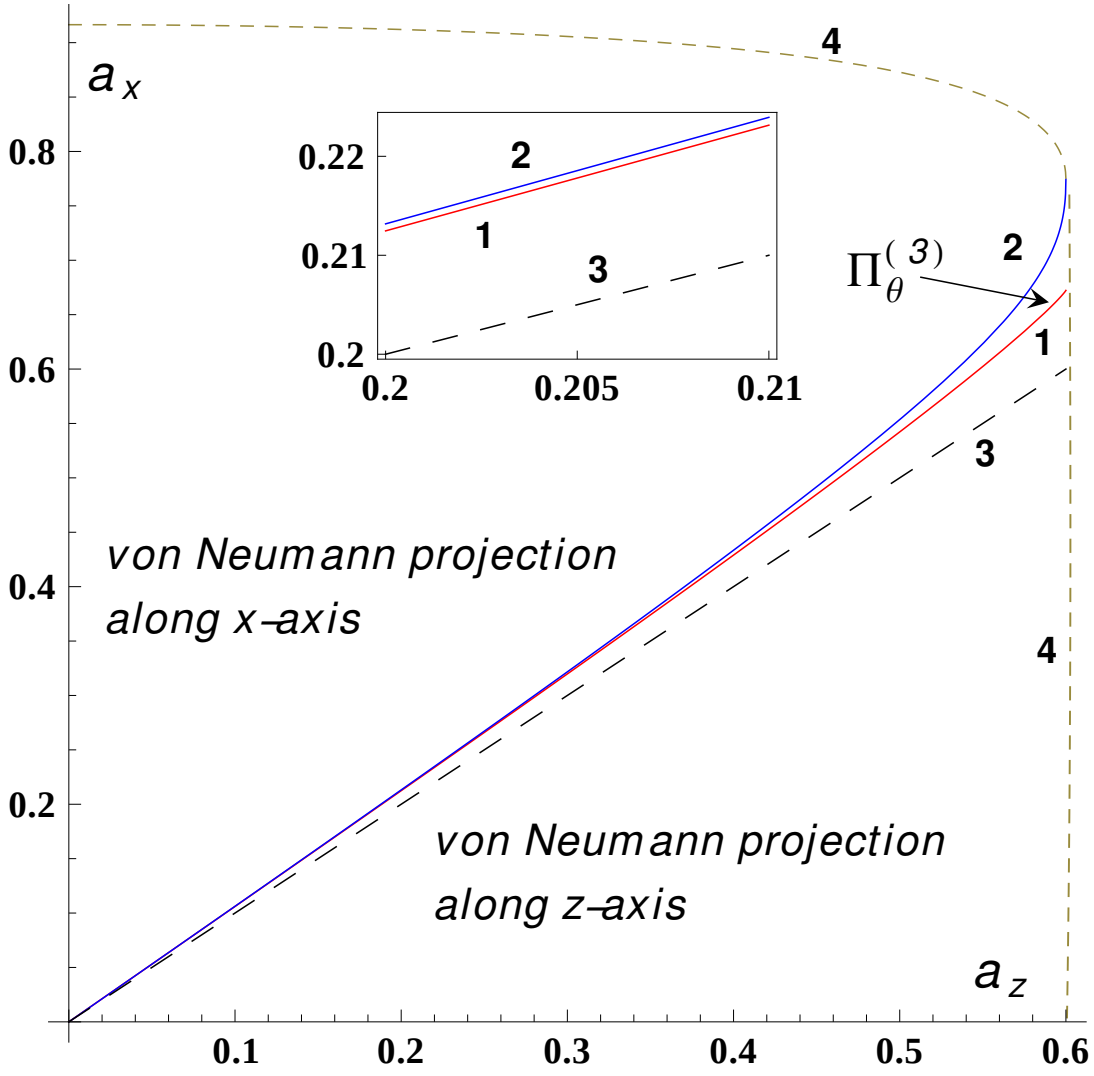

Figure 3.5: Showing the various measurement schemes across a slice (the $a_x - a_z$ plane) of parameter space (of correlation ellipsoids) with $z_c = 0.4$. We see that only for a tiny wedge-shaped region marked $\Pi_\theta^{(3)}$, the region between $a^V(a_z, z_c)$ (1) and $a^H(a_z, z_c)$ (2), one can expect a 3-element POVM. Region above (2) corresponds to a von Neumann measurement along the x-axis and the region below curve (1) corresponds to a von Neumann measurement along the z-axis. Curves marked (4) depict the boundary of allowed values for a_z, a_x. The curve (3) is the line $a_z = a_x$. The inset shows curves (1), (2) and (3) for $a_x \in [0.2, 0.21]$.

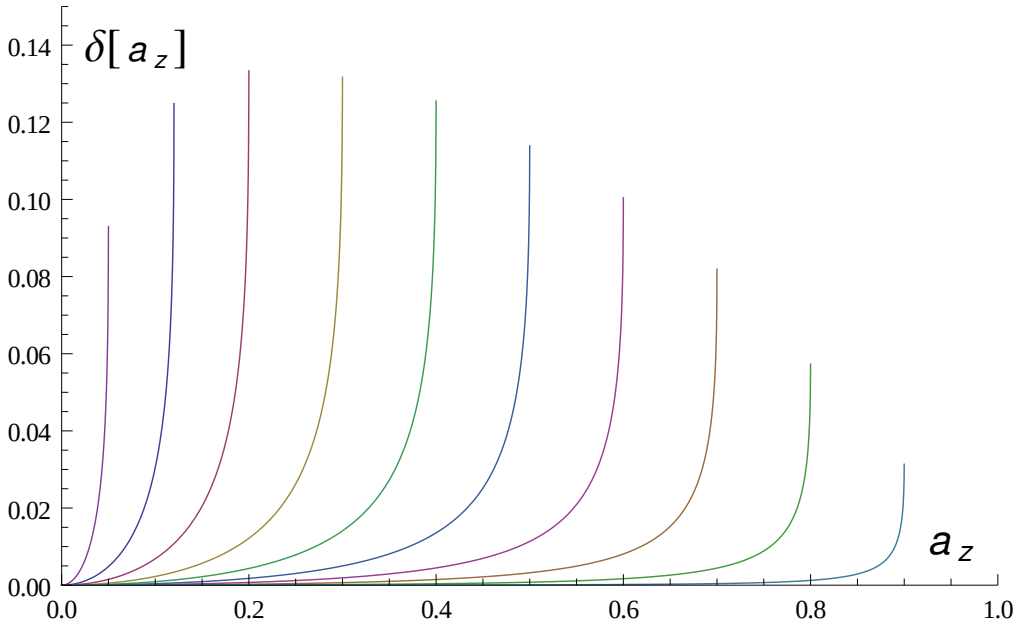

Figure 3.6: Showing $\delta(a_z)$ for decreasing values of z_c from left to right. The first curve corresponds to $z_c = 0.95$ and the last curve to $z_c = 0.1$. We see that size of the 'wedge'-shaped region (Fig. 3.5) first increases and then decreases with increasing z_c.

x-axis, and never the z-axis.

We also note that the range of values of a_x for a fixed (a_z, z_c) where the potential three-element POVM can exist increases with increasing a_z. Let us define a parameter δ as $\delta(a_z, z_c) = a_x^H(a_z, z_c) - a_x^V(a_z, z_c)$ which captures the extent of region bounded by curves (1) and (2) in Fig. 3.5. This object is shown in Fig. 3.6. We see that the range of values of a_x for which a three-element POVM exists first increases with increasing z_c and then decreases.

An example : We now evaluate quantum discord for a one-parameter family of states we

construct and denote by $\hat{\rho}(a)$. The Mueller matrix associated with $\hat{\rho}(a)$ is chosen as :

$$M(a) = \begin{bmatrix} 1 & 0 & 0 & y \\ 0 & a(1-y^2)^{1/2} & 0 & 0 \\ 0 & 0 & 0.59(1-y^2)^{1/2} & 0 \\ 0.5 & 0 & 0 & 0.58+0.4y \end{bmatrix}, \tag{3.39}$$

where $a \in [0.59, 0.7]$ and $y = 0.1/0.58$. The ellipsoid parameters for our class of states is given by $(a_x, a_y, a_z, z_c, z_I) = (a, 0.59, 0.58, 0.4, 0.5)$. The class of states differ only in the parameter a_x which changes as the parameter a is varied in the chosen interval. Using the optimal measurement scheme outlined above and in the earlier Section, we compute $S^A_{\min}$ and quantum discord. The values are displayed in Fig. 3.7 in which $S^A_{\min}$ is denoted by curve (1) and quantum discord by curve (4). An over-estimation of quantum discord by restricting to von Neumann measurements along x or z-axis is shown in curve (3) for comparison with the optimal three-element POVM. The point E denotes the change in the measurement from z-axis projection to a three-element POVM and point F denotes a change from the three-element POVM scheme to the x-axis von Neumann measurement.

This transition is clearly shown in Fig. 3.8. We see that had one restricted to only the von Neumann measurement along the z-axis or the x-axis, one would obtain a 'kink' in the value for quantum discord. Whereas, the optimal three-element scheme returns a gradual change in the value of quantum discord as we change the parameter a. The curves (3) and (4) will only merge for the value $z_c = 0$ and this aspect will be detailed in a later Section. This behaviour of quantum discord is generic to any non-zero value of the center z_c of the correlation ellipsoid.

Purification and EoF : The Koashi-Winter theorem or relation [242] shows that the classical correlation of a given bipartite state $\hat{\rho}_{AB}$ is related to the entanglement of formation

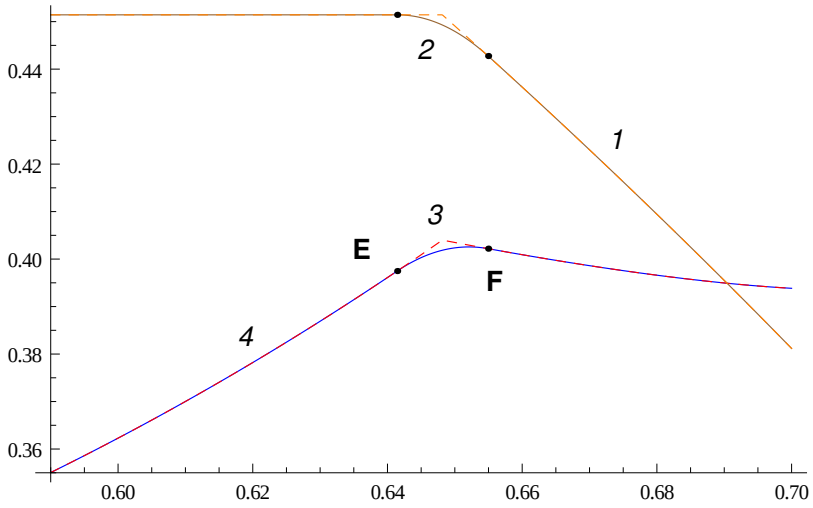

Figure 3.7: Showing $S^A_{\min}$ [curve (1)] and quantum discord [curve (4)] for a one-parameter family of states $\hat{\rho}(a)$. The ellipsoid corresponding to $\hat{\rho}(a)$ has parameters $(a_x, a_y, a_z, z_c, z_I) = (a, 0.59, 0.58, 0.4, 0.5)$ where $a \in [0.59, 0.7]$. Point E denotes the change of the optimal measurement from a von Neumann measurement along the z-axis to a three-element POVM, while point F denotes the change of the optimal measurement from a three-element POVM to a von Neumann measurement along the x-axis, with increasing values of the parameter a. The curve (3) (or (2)) denotes the over(under)-estimation of quantum discord (or $S^A_{\min}$) by restricting the measurement scheme to a von Neumann measurement along the z or x-axis. This aspect is clearly brought out in the following Fig. 3.8.

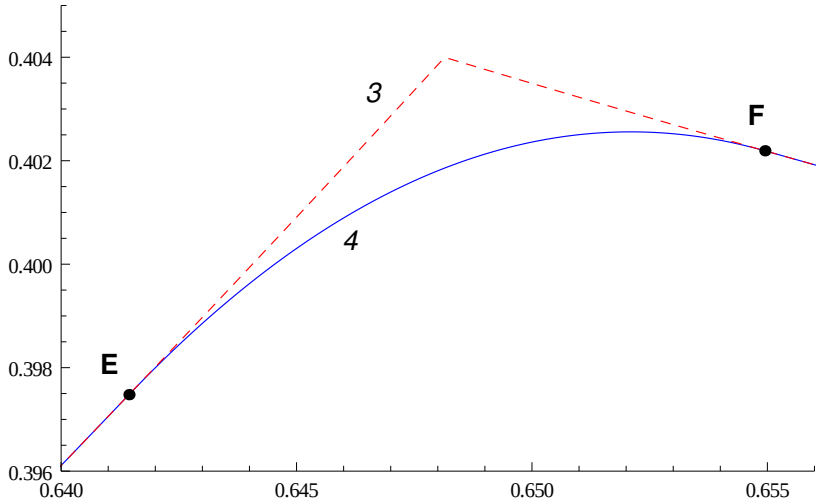

Figure 3.8: Showing quantum discord [curve (4)] with increasing a_x when there is a transition of the measurement scheme from the von Neumann measurement along the z-axis to the three-element scheme (E) and finally to the von Neumann measurement along the x-axis (F). The over-estimation of quantum discord is depicted in curve (3) where the measurement scheme is restricted to one of von Neumann measurements along the z or x-axis. We see a gradual change in quantum discord in contrast to the sharp change in the restricted case.

of the 'complimentary' state $\hat{\rho}_{CA}$. That is,

$$C(\hat{\rho}_{AB}) = S(\hat{\rho}_A) - E_F(\hat{\rho}_{CA}). \tag{3.40}$$

Comparing with the definition of $S^A_{\min}$ in Eq. (1.57), we see that

$$S^A_{\min}(\hat{\rho}_{AB}) = E_F(\hat{\rho}_{CA}). \tag{3.41}$$

In other words, the Koashi-Winter relation connects the (minimum average) conditional entropy post measurement of a bipartite state $\hat{\rho}_{AB}$ to the entanglement of formation of its complimentary state $\hat{\rho}_{CA}$ defined through purification of $\hat{\rho}_{AB}$ to pure state $|\phi_{C:AB}\rangle$.

The purification can be written as $|\phi_{C:AB}\rangle = \sum_{j=0}^{3} \sqrt{\lambda_j}|e_j\rangle \otimes |\psi_j\rangle$, $\{|e_j\rangle\}$ being orthonormal vectors in the Hilbert space of subsystem C. Now, the complimentary state $\hat{\rho}_{CA}$ results when subsystem B is simply discarded :

$$\begin{aligned}\hat{\rho}_{CA} &= \mathrm{Tr}_B[|\phi_{C:AB}\rangle\langle\phi_{C:AB}|] \\ &= \sum_{j,k=0}^{3} \sqrt{\lambda_j\lambda_k}|e_j\rangle\langle e_k| \otimes \mathrm{Tr}[|\psi_j\rangle\langle\psi_k|].\end{aligned} \tag{3.42}$$

It is easy to see that for the case of the two qubit X-states, the complimentary state belongs to a 2×4 system. Now that $S^A_{\min}$ is determined for all X-states by our procedure, using Eqs. (3.17), (3.18), (3.19) one can immediately write down the expressions for the entanglement of formation for the complimentary states corresponding to the entire 11-parameter family of X-states states using the optimal measurement scheme outlined in Sec. 3.5. We note in passing that examples of this connection for the particular cases of states such as rank-two two-qubit states and Bell-mixtures have been earlier studied in [243, 244].

3.7 Invariance group beyond local unitaries

Recall that a measurement element (on the B side) need not be normalized. Thus in constructing the correlation ellipsoid associated with a two-qubit state $\hat{\rho}_{AB}$, we gave as input to the Mueller matrix associated with $\hat{\rho}_{AB}$ an arbitrary four-vector in the positive solid light cone (corresponding to an arbitrary 2×2 positive matrix), and then normalized the output Stokes vector to obtain the image point on the correlation ellipsoid. It follows, on the one hand, that all measurement elements which differ from one another by positive multiplicative factors lead to the same image point on the correlation ellipsoid. On the other hand it follows that $a\,\hat{\rho}_{AB}$ has the same correlation ellipsoid as $\hat{\rho}_{AB}$, for all $a > 0$. As one consequence, it is not necessary to normalize a Mueller matrix to $m_{00} = 1$ as far as construction of the correlation ellipsoid is concerned.

The fact that construction of the correlation ellipsoid deploys the entire positive solid light cone of positive operators readily implies that *the ellipsoid inherits all the symmetries of this solid light cone*. These symmetries are easily enumerated. Denoting by ψ_1, ψ_2 the components of a vector $|\psi\rangle$ in Bob's Hilbert space $\mathcal{H}_B$, a nonsingular linear transformation

$$J : \begin{pmatrix} \psi_1 \\ \psi_2 \end{pmatrix} \rightarrow \begin{pmatrix} \psi_1' \\ \psi_2' \end{pmatrix} = J \begin{pmatrix} \psi_1 \\ \psi_2 \end{pmatrix} \tag{3.43}$$

on $\mathcal{H}_B$ corresponds on Stokes vectors to the transformation $|\det J|\, L$ where L is an element of the Lorentz group $SO(3,1)$, and the factor $|\det J|$ corresponds to 'radial' scaling of the light cone. Following the convention of classical polarization optics, we may call J the *Jones matrix* of the (non-singular) local filtering [231, 233, 234]. When $(\det J)^{-1/2} J = L$ is polar decomposed, the positive factor corresponds to pure boosts of $SO(3,1)$ while the (local) unitary factor corresponds to the 'spatial' rotation subgroup $SO(3)$ of $SO(3,1)$ [231, 233, 234]. It follows that restriction of attention to the section $S_0 = 1$ confines the invariance group from $SO(3,1)$ to $SO(3)$.

The positive light cone is mapped onto itself also under inversion of all 'spatial' coordinates: $(S_0, \mathbf{S}) \to (S_0, -\mathbf{S})$. This symmetry corresponds to the Mueller matrix $T = \mathrm{diag}(1, -1, -1, -1)$, which is equivalent to $T_0 = \mathrm{diag}(1, 1, -1, 1)$, and hence corresponds to the transpose map on 2×2 matrices. In contradistinction to $SO(3,1)$, T_0 acts directly on the operators and cannot be realized or lifted as filtering on Hilbert space vectors; indeed, it cannot be realized as any physical process. Even so, it remains a symmetry of the positive light cone and hence of the correlation ellipsoid itself.

The full invariance group $\mathcal{G}$ of a correlation ellipsoid thus comprises two copies of the Lorentz group and the one-parameter semigroup of radial scaling by factor $a > 0$:

$$\mathcal{G} = \{SO(3,1),\ TSO(3,1) \approx SO(3,1)T,\ a\}. \tag{3.44}$$

All Mueller matrices MM_0 with $M_0 \in \mathcal{G}$ and fixed M correspond to one and the same correlation ellipsoid. In what follows we examine briefly the manner in which these invariances could be exploited for our purpose, and we begin with $SO(3,1)$.

The Jones matrix $J = \exp[\mu\sigma_3/2] = \mathrm{diag}(e^{\mu/2}, e^{-\mu/2})$ corresponds to the Lorentz boost

$$M_0(\mu) = c_\mu \begin{bmatrix} 1 & 0 & 0 & t_\mu \\ 0 & (c_\mu)^{-1} & 0 & 0 \\ 0 & 0 & (c_\mu)^{-1} & 0 \\ t_\mu & 0 & 0 & 1 \end{bmatrix} \tag{3.45}$$

along the third spatial direction on Stokes vectors. Here $c_\mu,\ t_\mu$ stand respectively for $\cosh\mu$ and $\tanh\mu$. To see the effect of this boost on the correlation ellipsoid, consider a Mueller matrix of the form (3.12) with $m_{03} = 0$ so that $m_{11} = a_x$, $m_{33} = a_z$, $m_{22} = \pm a_y$ and $z_c = m_{30}$.

Absorbing the scale factor c_μ in Eq. (3.45) into the solid light cone, we have

$$MM_0(\mu) = \begin{bmatrix} 1 & 0 & 0 & t_\mu \\ 0 & m_{11}/c_\mu & 0 & 0 \\ 0 & 0 & m_{22}/c_\mu & 0 \\ m_{30} + m_{33}\, t_\mu & 0 & 0 & m_{33} + m_{30}\, t_\mu \end{bmatrix}. \tag{3.46}$$

With the help of (3.26) we immediately verify that a_x, a_y, a_z, and z_c associated with $MM_0(\mu)$ are exactly those associated with M with no change whatsoever, consistent with the fact that we expect M and $MM_0(\mu)$ to have the same correlation ellipsoid. Only z_I, the image of identity, changes from m_{30} to $m_{30} + m_{33}\, t_\mu$: as t_μ varies over the permitted open interval $(-1, 1)$, the point I varies linearly over the open interval $(z_c - a_z,\, z_c + a_z)$. Thus, *it is the Lorentz boost on the B side which connects states having one and the same correlation ellipsoid, but different values of* z_I.

As an illustration of this connection, we go back to Fig. 3.5 and consider a correlation ellipsoid in the interior of the wedge region between curves (1) and (2) of Fig. 3.5. We recall that a point in this region is distinguished by the fact that for states corresponding to this point the optimal POVM could *potentially* be a three-element POVM, but whether a three element POVM or a horizontal projection actually turns out to be the optimal one for a state requires the value of z_I as additional information on the state, beyond the correlation ellipsoid. The behaviour of classical correlation, quantum discord, and mutual information as the Lorentz boost on the B side sweeps z_I across the full interval $(z_c - a_z, z_c + a_z)$ is presented in Fig. 3.9. We repeat that the entire Fig. 3.9 corresponds to one fixed point in Fig. 3.5.

Remark : Any entangled two-qubit pure state can be written as

$$|\psi\rangle_{AB} = (\mathbb{1} \otimes J)\, |\psi_{\max}\rangle, \tag{3.47}$$

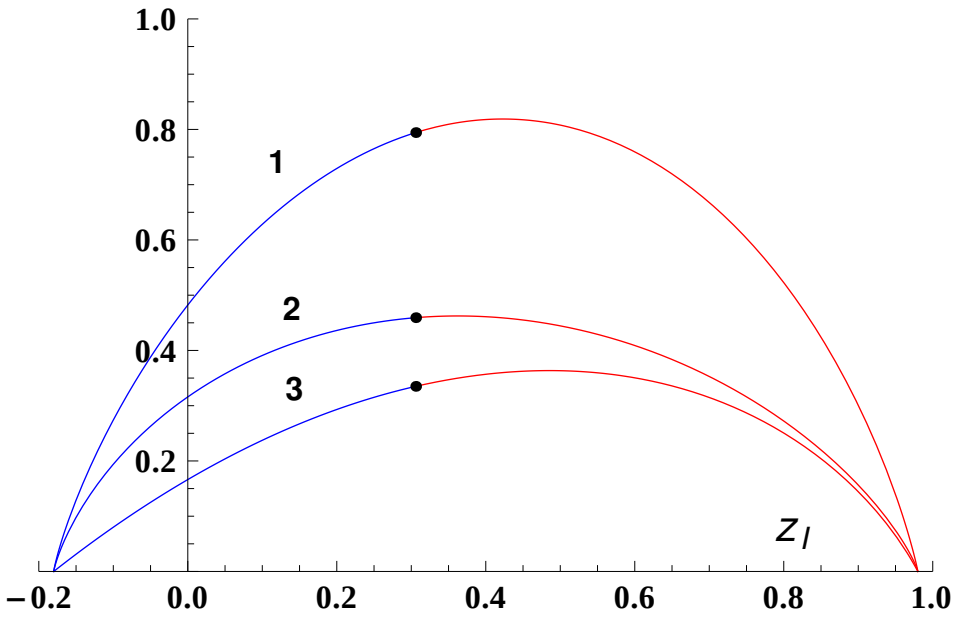

Figure 3.9: Showing mutual information (1), quantum discord (2) and classical correlation (3) as a function of z_I for the ellipsoid parameters $(a_z, z_c, a_x) = (0.58, 0.4, 0.65)$ and $z_0 = 0.305919$. For $z_I \leq z_0$, the optimal measurement is a von Neumann measurement along the x-axis, and for $z_I > z_0$ the optimal measurement is a three-element POVM.

where the Jones matrix J is non-singular and $|\psi_{\max}\rangle$ is a Bell state. Since the associated $SO(3,1)$ does not affect the correlation ellipsoid, the ellipsoid corresponding to $|\psi\rangle_{AB}$ is the same as that of the Bell state, and thereby it is the full Bloch sphere. Hence, $S^A_{\min}$ trivially evaluates to zero. So we see that for all two-qubit pure states $I(\hat{\rho}_{AB}) = 2C(\hat{\rho}_{AB}) = 2D(\hat{\rho}_{AB}) = 2E(\hat{\rho}_{AB})$. ■

Remark : It is useful to make two minor observations before we leave the present discussion of the role of $SO(3,1)$. First, it is obvious that a bipartite operator $\hat{\rho}_{AB}$ is positive if and only if its image under any (nonsingular) local filtering J is positive. This, combined with the fact that the location of z_I inside the correlation ellipsoid can be freely moved around using local filtering, implies that the location of z_I has no role to play in the characterization of positivity of $\hat{\rho}_{AB}$ given in (3.15), (3.16). Consequently, in forcing these positivity requirements on the correlation ellipsoid we are free to move, without loss of generality, to the simplest case corresponding to $z_I = z_c$ or $m_{03} = 0$.

Secondly, since determinant of an $SO(3,1)$ matrix is positive, we see that local filtering does not affect the signature of $\det M$, and hence it leaves unaffected the signature of the correlation ellipsoid itself : Ω^+ and Ω^- remain separately invariant under $SO(3,1)$. ■

The case of the spatial inversion T, to which we now turn our attention, will prove to be quite different on both counts. It is clear that the effect of $T_0 : M \to MT_0$ on an X-state Mueller matrix is to transform m_{22} to $-m_{22}$, leaving all other entries of M invariant. Since the only way m_{22} enters the correlation ellipsoid parameters in (3.25) is through $a_y = |m_{22}|$, it follows that the correlation ellipsoid itself is left invariant, but its signature gets reversed : $\det MT_0 = -\det M$. This reversal of signature of the ellipsoid has important consequences.

As explained earlier during our discussion of the role of $SO(3,1)$ we may assume, without loss of generality, $z_I = z_c$ or, equivalently, $m_{03} = 0$. The positivity conditions (3.15), (3.16) then read as the following requirements on the ellipsoid parameters :

$$(1 + a_z)^2 - z_c^2 \geq (a_x + a_y)^2, \tag{3.48}$$

$$(1 - a_z)^2 - z_c^2 \geq (a_x - a_y)^2, \tag{3.49}$$

in the case $M \in \Omega^+$, and

$$(1 + a_z)^2 - z_c^2 \geq (a_x - a_y)^2, \tag{3.50}$$

$$(1 - a_z)^2 - z_c^2 \geq (a_x + a_y)^2, \tag{3.51}$$

in the case $M \in \Omega^-$. But (3.50) is manifestly weaker than (3.51) and hence is of little consequence. The demand that MT_0 too correspond to a physical state requires

$$(1 + a_z)^2 - z_c^2 \geq (a_x - a_y)^2, \tag{3.52}$$

$$(1 - a_z)^2 - z_c^2 \geq (a_x + a_y)^2, \tag{3.53}$$

in the case $M \in \Omega^+$, and

$$(1 + a_z)^2 - z_c^2 \geq (a_x + a_y)^2, \tag{3.54}$$

$$(1 - a_z)^2 - z_c^2 \geq (a_x - a_y)^2, \tag{3.55}$$

in the case of $M \in \Omega^-$.

Now, in the case of $M \in \Omega^+$, (3.52) is weaker than (3.48) and hence is of no consequence, but (3.53) is stronger than and subsumes *both* (3.48) and (3.49). In the case $M \in \Omega^-$ on the other hand both (3.54) and (3.55) are weaker than (3.51). These considerations establish the following :

1. If $M \in \Omega^-$, its positivity requirement is governed by the single condition (3.51) and, further, MT_0 certainly corresponds to a physical state in Ω^+.

2. If $M \in \Omega^+$, then $MT_0 \in \Omega^-$ is physical if and only if the additional condition (3.53) which is the same as (3.51) is met.

Since T_0 is the same as partial transpose on the B side, we conclude that a correlation ellipsoid corresponds to a separable state if and only if (3.51) is met, and it may be emphasised that this statement is independent of the signature of the ellipsoid. Stated differently, those correlation ellipsoids in Ω^+ whose signature reversed version are not present in Ω^- correspond to entangled states. In other words, the set of entangled X-states constitute precisely the Ω^- complement of Ω^+.

Finally, the necessary and sufficient condition $(1 - a_z)^2 - z_c^2 \geq (a_x + a_y)^2$ for separability can be used to ask for correlation ellipsoid of maximum volume that corresponds to a separable state, for a given z_c. In the case $z_c = 0$, it is easily seen that the maximum volume obtains for $a_x = a_y = a_z = 1/3$, and evaluates to a fraction $1/27$ of the volume of

the Bloch ball. For $z_c \neq 0$, this fractional volume $V(z_c)$ can be shown to be

$$V(z_c) = \frac{1}{54}(2 - \sqrt{1 + 3z_c^2})^2(1 + \sqrt{1 + 3z_c^2}), \tag{3.56}$$

and corresponds to

$$a_x = a_y = \frac{[(2 - \sqrt{1 + 3z_c^2})(1 + \sqrt{1 + 3z_c^2})]^{1/2}}{3\sqrt{2}}, \quad a_z = \frac{2 - \sqrt{1 + 3z_c^2}}{3}. \tag{3.57}$$

It is a monotone decreasing function of z_c. Thus Ω^- has no ellipsoid of fractional volume $> 1/27$.

Remark : It is clear that any X-state whose ellipsoid degenerates into an elliptic disc necessarily corresponds to a separable state. This sufficient separability condition may be contrasted with the case of discord wherein the ellipsoid has to doubly degenerate into a line segment for nullity of quantum discord to obtain

3.8 Comparison with the work of Ali, Rau, and Alber

In this Section we briefly contrast our approach and results with those of the famous work of Ali, Rau, and Alber (ARA) [220], whose principal claim comprises two parts :

C1 : Among all von Neumann measurements, either the horizontal or the vertical projection always yields the optimal classical correlation and quantum discord.

C2 : The values thus computed remain optimal even when general POVM's are considered.

As for the second claim, the main text of ARA simply declares "The Appendix shows how we may generalize to POVM to get final compact expressions that are simple extensions

of the more limited von Neumann measurements, thereby *yielding the same value* for the maximum classical correlation and discord." The Appendix itself seems not to do enough towards validating this claim. It begins with "Instead of von Neumann projectors, consider more general POVM. For instance, choose three orthogonal unit vectors mutually at 120°,

$$\hat{s}_{0,1,2} = [\hat{z}, (-\hat{z} \pm \sqrt{3}\hat{x})/2], \tag{3.58}$$

and corresponding projectors $\cdots$." [It is not immediately clear how 'orthogonal' is to be reconciled with 'mutually as 120°']. Subsequent reference to their Eq. (11) possibly indicates that ARA have in mind two more sets of such *three orthogonal unit vectors mutually at* 120° related to (3.58) through $SU(2)$ rotations. In the absence of concrete computation aimed at validating the claim, one is left to wonder if the second claim (C2) of ARA is more of an assertion than deduction.

We now know, however, that the actual situation in respect of the second claim is much more subtle : the optimal three-element POVM is hardly of the *three orthogonal unit vectors mutually at* 120° type and, further, when a three-element POVM is required as the optimal one, there seems to be no basis to anticipate that it would yield 'the same value for the maximum classical correlation and discord'.

Admittedly, the present work is not the first to discover that ARA is not the last word on quantum discord of X-states. Several authors have pointed to examples of X-states which fail ARA [221, 222, 225, 227–229, 245]. But these authors have largely been concerned with the second claim (C2) of ARA. In contradistinction, our considerations below focuses on the first one (C1). In order that it be clearly understood as to what the ARA claim (C1) is not, we begin with the following three statements :

S1 : If von Neumann projection proves to be the optimal POVM, then the projection is either along the x or z direction.

S2 : von Neumann projection along the x or z direction always proves to be the optimal POVM.

S3 : von Neumann projection along either the x or z direction proves to be the best among all von Neumann projections.

Our analysis has confirmed that the first statement (S1) is absolutely correct. We also know that the second statement (S2) is correct except for a very tiny fraction of states corresponding to the wedge-like region between curves (1) and (2) in Fig. 3.5.

The first claim (C1) of ARA corresponds, however, to neither of these two but to the third statement (S3). We begin with a counter-example to prove that this claim (S3) is non-maintainable. The example corresponds to the ellipsoid parameters $(a_x, a_y, a_z, z_c) = (0.780936, 0.616528, 0.77183, 0.122479)$. These parameters, together with $z_I = 0.3$, fully specify the state in the canonical form, and the corresponding Mueller matrix

$$M = \begin{pmatrix} 1 & 0 & 0 & 0.23 \\ 0 & 0.76 & 0 & 0 \\ 0 & 0 & 0.6 & 0 \\ 0.3 & 0 & 0 & 0.8 \end{pmatrix}. \tag{3.59}$$

The parameter values verify the positivity requirements. Further, it is seen that $M \in \Omega^+$ and corresponds to a nonseparable state. The x-z section of the correlation ellipsoid corresponding to this example is depicted in Fig. 3.10.

Let us denote by $S^A_{vN}(\theta)$ the average conditional entropy post von Neumann measurement Π_θ parametrized by angle θ :

$$\Pi_\theta = \left\{(1, \sin\theta, 0, \cos\theta)^T,\ (1, -\sin\theta, 0, -\cos\theta)^T\right\},\quad 0 \le \theta \le \pi/2. \tag{3.60}$$

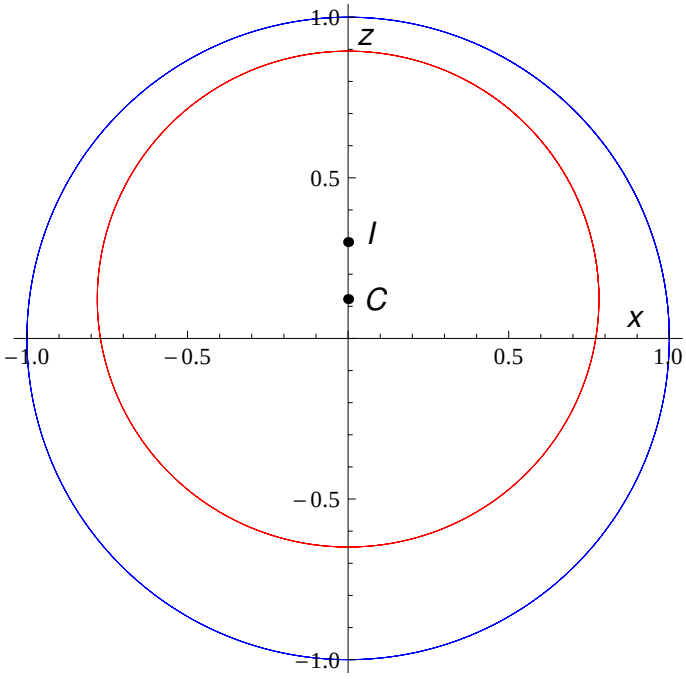

Figure 3.10: Showing the x-z cross-section of the ellipsoid associated with the Mueller matrix in (3.59).

It is clear that the output states are at distances $r(\theta)$, $r^{'}(\theta)$ with respective conditional probabilities $p(\theta)$, $p^{'}(\theta)$:

$$\begin{aligned} r(\theta) &= \frac{\sqrt{(m_{11}\,\sin\theta)^2 + (m_{30} + m_{33}\,\cos\theta)^2}}{1 + m_{03}\,\cos\theta}, \\ r^{'}(\theta) &= \frac{\sqrt{(m_{11}\,\sin\theta)^2 + (m_{30} - m_{33}\,\cos\theta)^2}}{1 - m_{03}\,\cos\theta}, \\ p(\theta) &= \frac{1 + m_{03}\,\cos\theta}{2}, \quad p^{'}(\theta) = \frac{1 - m_{03}\,\cos\theta}{2}. \end{aligned} \tag{3.61}$$

Thus $S^{A}_{vN}(\theta)$ evaluates to

$$\begin{aligned} S^{A}_{vN}(\theta) = \frac{1}{2}\Big[&S_2(r(\theta)) + S_2(r^{'}(\theta)) \\ &+ m_{03}\,\cos\theta\,(S_2(r(\theta)) - S_2(r^{'}(\theta)))\Big]. \end{aligned} \tag{3.62}$$

The behaviour of $S^{A}_{vN}(\theta)$ as a function of θ is shown in Fig. 3.11, and it is manifest that the optimal von Neumann obtains *neither at* $\theta = 0$ *nor at* $\pi/2$, *but at* $\theta = 0.7792$ *radians*.

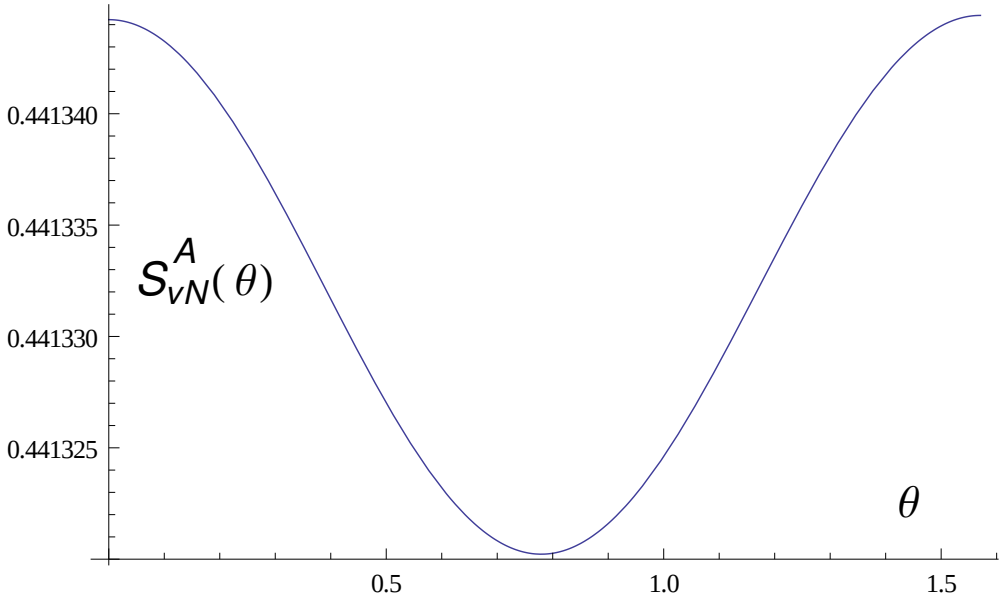

Figure 3.11: Showing the conditional entropy $S^A_{vN}(\theta)$ resulting from von Neumann measurements for the example in (3.59).

More strikingly, it is not only that neither $\theta = 0$ or $\pi/2$ is the best, but both are indeed the worst in the sense that von Neumann projection along any other direction returns a better value!

We know from our analysis in Section 3.6 that if the von Neumann measurement indeed happens to be the optimal POVM, it can not obtain for any angle other than $\theta = 0$ or $\pi/2$. Thus, the fact that the best von Neumann for the present example corresponds to neither angle is already a sure signature that a three-element POVM is the optimal one for the state under consideration. Prompted by this signature, we embed the state under consideration in a one-parameter family with fixed $(a_z, a_y, z_c) = (0.616528, 0.77183, 0.122479)$ and z_I, and a_x varying over the range $[0.7803, 0.7816]$. The results are shown in Fig. 3.12. Curve (1) and curve (2) correspond respectively to the horizontal and vertical von Neumann projections, whereas curve (3) corresponds to the optimal three-element POVM. We emphasise that curve (3) is not asymptotic to curves (1) or (2), but joins them at G and E respectively. Our example of Eq. (3.59) embedded in this one-parameter family is highlighted by points A, B, F. This example is so manufactured that S^A_{vN} computed by the

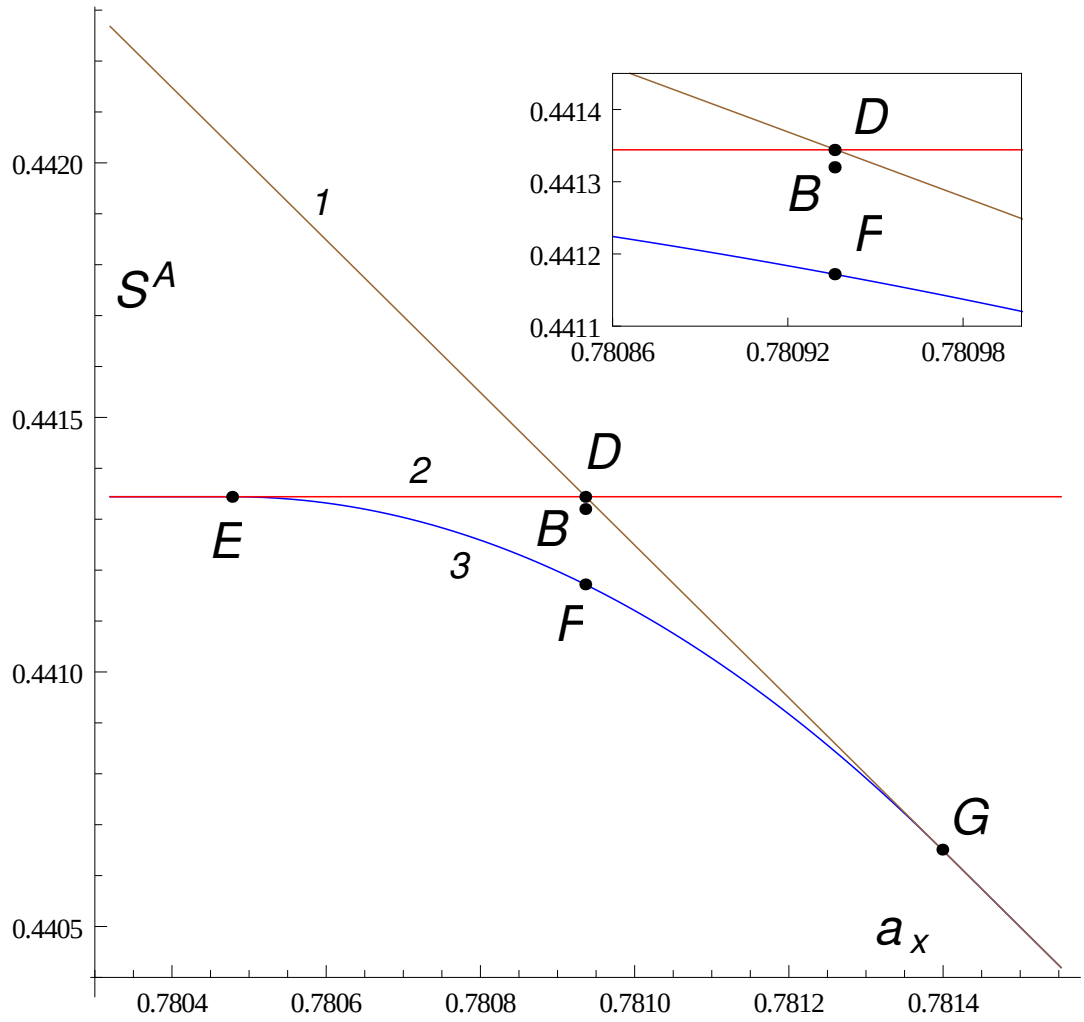

Figure 3.12: Showing the entropy variation with respect to variation of a_x in $[0.78032, 0.781553]$, with (a_y, a_z, z_c) fixed at $(0.616528, 0.77183, 0.122479)$. Curve (1) depicts S^A_{vN} for von Neumann measurement along $\theta = \pi/2$, the constant line [curve (2)] to a von Neumann measurement along $\theta = 0$, and curve (3) to $S^A_{\min}$ resulting from the three element POVM scheme. The example in ((3.59)) corresponds to $a_x = 0.780936$. The inset compared the various schemes of the example in (3.59). D refers to the a measurement restricted only to the von Neumann projection along z or x-axis, B to the best von Neumann projection, and F to the optimal three-element measurement.

Scheme	Elements	Optimal value	S^A
von Neumann	σ_x or σ_z	equal	0.441344
von Neumann	$\Pi_\theta^{vN}, \quad \theta \in [0, \pi/2]$	$\theta_{\text{opt}} = 0.779283$	0.44132
3-element POVM	$\Pi_\theta^{(3)}, \quad \theta \in [0, \pi/2]$	$\theta_{\text{opt}} = 1.02158$	0.441172

Table 3.1: Showing a comparison of the von Neumann and the three-element POVM schemes for the example in Eq. (3.59).

horizontal projection equals the value computed by the vertical projection, and denoted by point D. The point B corresponds to S^A_{vN} evaluated using the best von Neumann, and F to the one computed by the (three-element) optimal POVM. It may be noted that D and B are numerically quite close as highlighted by the inset. A numerical comparison of these values is conveniently presented in Table 3.1.

It is seen from Fig. 3.12 that vertical von Neumann is the optimal POVM upto the point E (i.e. for $a_x \leq 0.780478$), from E all the way to G the three-element POVM $\Pi_\theta^{(3)}$ is the optimal one, and beyond G ($a_x \geq 0.781399$) the horizontal von Neumann is the optimal POVM. The continuous evolution of the parameter θ in $\Pi_\theta^{(3)}$ of Eq. (3.30) as one moves from E to G is shown in Fig. 3.13. Shown also is the continuous manner in which the probability $p_0(\theta)$ in Eq. (3.30) continuously varies from 0.5 to zero as a_x varies over the range from E to G.

In order to reconcile ARA's first claim (S3 above) with our counter-example we briefly reexamine their very analysis leading to the claim. As we shall see the decisive stage of their argument is symmetry-based or group theoretical in tenor. It is therefore unusual that they carry around an extra baggage of irrelevant phase parameters, not only in the main text but also in the reformulation presented in their Appendix : the traditional first step in symmetry-based approach is to transform the problem to its simplest form (often called the canonical form) without loss of generality. Their analysis beings with parametrization of von Neumann measurements as [their Eq. (11)]

$$B_i = V \Pi_i V^\dagger, \quad i = 0, 1 \tag{3.63}$$

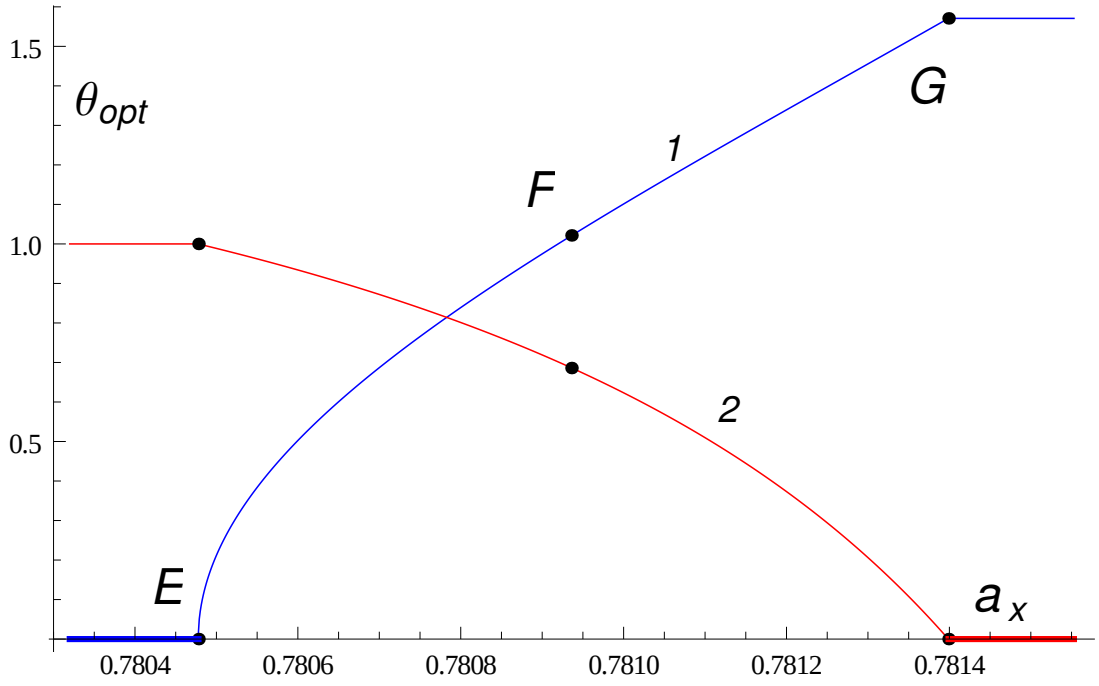

Figure 3.13: Showing the optimal $\theta = \theta_{\rm opt}$ of $\Pi_\theta^{(3)}$ [curve(1)] resulting in $S^A_{\rm min}$ depicted as curve (3) in Fig. 3.12. Curve (2) shows the probability (scaled by a factor of 2) $2p_0(\theta_{\rm opt})$ of the conditional state corresponding to input POVM element $(1,0,0,1)^T$.

where $\Pi_i = |i\rangle\langle i|$ is the projector on the computation state $|i\rangle \in \{|0\rangle, |1\rangle\}$ and $V \in SU(2)$. With the representation $V = t\mathbb{1} + i\vec{y}.\vec{\sigma}$, $t^2 + y_1^2 + y_2^2 + y_3^2 = 1$ they note that three of these four parameters t, y_1, y_2, y_3 are *independent*. Inspired by their Ref. [15] (our Ref. [219]), ARA recast t, y_1, y_2, y_3 into four new parameters m, n, k, ℓ and once again emphasize that k, m, n are three *independent* parameters describing the manifold of von Neumann measurements.

Remark: It is obvious that every von Neumann measurement on a qubit is fully specified by a pure state, and hence the manifold of von Neumann measurements can be no larger than $\mathcal{S}^2$, the Bloch sphere. Indeed, this manifold is even 'smaller': it coincides with the real projective space $\mathcal{RP}^2 = \mathcal{S}^2/\mathcal{Z}_2$ of diameters in $\mathcal{S}^2$, since a pure state and its orthogonal partner define *one and the same* von Neumann measurement. In any case, it is not immediately clear in what sense could this two-manifold be described by three

'independent' parameters. ■

Remark: We should hasten to add, for completeness, that ARA introduce subsequently, in an unusually well cited *erratum* [246], another identity

$$m^2 + n^2 = klm \tag{3.64}$$

which they claim to be independent of $t^2 + y_1^2 + y_2^2 + y_3^2 = 1$, and hence expect it to reduce the number of independent variables parametrizing the manifold of von Neumann measurements from three to two. To understand the structure of this new identity, define two complex numbers $\alpha = t - iy_3, \beta = y_1 + iy_2$. Then $k = |\alpha|^2$, $\ell = |\beta|^2$, $m = (\mathrm{Re}\alpha\beta)^2$, and $n = (\mathrm{Re}\alpha\beta)\,(\mathrm{Im}\alpha\beta)$ so that the ARA identity Eq. (3.64) reads

$$(\mathrm{Re}\alpha\beta)^4 + (\mathrm{Re}\alpha\beta)^2\,(\mathrm{Im}\alpha\beta) = |\alpha\beta|^2(\mathrm{Re}\alpha\beta)^2, \tag{3.65}$$

showing that it is indeed independent of $k + \ell = 1$ as claimed by ARA. Indeed, it is simply the Pythagorean theorem $|z|^2 = (\mathrm{Re}z)^2 + (\mathrm{Im}z)^2$ valid for any complex number z puffed up to the appearance of an eighth degree real homogeneous form. It is unlikely that such an *universal* identity, valid for any four numbers, would ever aid in reducing the number of independent parameters. Not only ARA, but also the large number of works which cite this erratum, seem to have missed this aspect of the ARA identity (3.64). ■

Returning now to the clinching part of the ARA analysis, after setting up the expression for the conditional entropy as a function of their independent variables k, m, n they correctly note that it could be minimized "by setting equal to zero its partial derivatives with respect to k, m and n." Rather than carrying out this step, however, they prefer a short cut in the form of a symmetry argument. They '*observe*' that the problem has a symmetry (this is the symmetry of inversion about the z-axis which we used in Section 3.5 to simplify the optimization problem), and then use the *unusual symmetry argument* that if

a problem has a symmetry its solution *ought to be* invariant under that symmetry. Obviously, one knows in advance that the only von Neumann projections that are invariant under the symmetry under consideration are the vertical or z-projection and the horizontal projection, the latter meaning x or y-projection according as $a_x > a_y$ or $a_y > a_x$. This version of symmetry argument is unusual, since the familiar folklore version reads : *if a problem has a symmetry, its solution ought to be covariant (and not necessarily invariant) under the symmetry*. In any case, unless the ARA version of symmetry argument be justified as arising from some *special aspect* of the problem under consideration, its deployment would amount to assuming a priori that either z or x-projection is the best von Neumann; but then this assumption is precisely the claim S3 ARA set out to prove as the very central result of their work.

Remark : The ARA version of symmetry argument would remain justified if it were the case that the problem is expected, from other considerations, to have a *unique* solution. This happens, for instance, in the case of *convex optimization*. But von Neumann measurements *do not form a convex set* and hence the ARA problem of optimization over von Neumann measurement is not one of convex optimization. Thus demanding a unique solution in their case would again amount to an a priori assumption equivalent to the theorem they set out to prove.

3.9 X-states with vanishing discord

Many authors have considered methods to enumerate the zero discord X-states [206, 207, 209]. Our analysis below is directly based on the very definition of vanishing discord and hence is elementary; more importantly, it leads to an *exhaustive* classification of these states, correcting an earlier claim. Any generic two-qubit state of vanishing quantum

discord can be written as [65]

$$\hat{\rho}_{AB} = U_A|0\rangle\langle 0|U_A^\dagger \otimes p_1\hat{\rho}_{B1} + U_A|1\rangle\langle 1|U_A^\dagger \otimes p_2\hat{\rho}_{B2}, \tag{3.66}$$

with $p_1,\ p_2 \geq 0$, $p_1 + p_2 = 1$, the measurements being assumed performed on subsystem A. We may write

$$p_1\hat{\rho}_{B1} = \begin{bmatrix} a_1 & b_1 \\ b_1^* & c_1 \end{bmatrix},\ \ p_2\hat{\rho}_{B2} = \begin{bmatrix} a_2 & b_2 \\ b_2^* & c_2 \end{bmatrix},$$
$$U_A = \begin{bmatrix} \alpha & \beta \\ -\beta^* & \alpha^* \end{bmatrix} \in SU(2). \tag{3.67}$$

Clearly, the reduced state of subsystem B is $p_1\hat{\rho}_{B1}+p_2\hat{\rho}_{B2}$, and that of A equals $U_A\left(p_1|0\rangle\langle 0|+ p_2|1\rangle\langle 1|\right)U_A^\dagger$. We now combine this nullity condition with the demand that the state under consideration be an X-state in the canonical form (3.11). From the off-diagonal blocks of $\hat{\rho}_{AB}$ we immediately see that $a_1 = a_2$ and $c_1 = c_2$. $\mathrm{Tr}\,\hat{\rho}_{AB} = a_1 + c_1 + a_2 + c_2 = 1$ implies $a_1 + c_1 = 1/2 = a_2 + c_2$. Vanishing of the 01 and 23 elements of $\hat{\rho}_{AB}$ forces the following constraints :

$$|\alpha|^2 b_1 + |\beta|^2 b_2 = 0,$$
$$|\alpha|^2 b_2 + |\beta|^2 b_1 = 0. \tag{3.68}$$

These imply in turn that either $|\alpha| = |\beta| = 1/\sqrt{2}$ or $b_1 = b_2 = 0$. The first case of $|\alpha| = |\beta| = 1/\sqrt{2}$ forces $b_2 = -b_1$, and we end up with a two-parameter family of zero

discord states

$$\hat{\rho}^A(a,b) = \frac{1}{4}\begin{pmatrix} 1+a & 0 & 0 & b \\ 0 & 1-a & b & 0 \\ 0 & b & 1+a & 0 \\ b & 0 & 0 & 1-a \end{pmatrix}$$
$$= \frac{1}{4}\left[\sigma_0 \otimes \sigma_0 + a\sigma_0 \otimes \sigma_3 + b\sigma_1 \otimes \sigma_1\right]. \tag{3.69}$$

Positivity of $\hat{\rho}^A(a,b)$ places the constraint $a^2 + b^2 \leq 1$, a disc in the $(\sigma_0 \otimes \sigma_3, \sigma_1 \otimes \sigma_1)$ plane. The case $b = 0$ corresponds to the product state

$$\hat{\rho}^{AB}(a) = \frac{1}{4}\mathbb{1} \otimes \begin{bmatrix} 1+a & 0 \\ 0 & 1-a \end{bmatrix}. \tag{3.70}$$

If instead the measurement was performed on the B subsystem, then it can be easily seen that similar arguments can be used to arrive at the zero discord states

$$\hat{\rho}^B(a,b) = \frac{1}{4}\begin{pmatrix} 1+a & 0 & 0 & b \\ 0 & 1+a & b & 0 \\ 0 & b & 1-a & 0 \\ b & 0 & 0 & 1-a \end{pmatrix},$$
$$= \frac{1}{4}\left[\sigma_0 \otimes \sigma_0 + a\sigma_3 \otimes \sigma_0 + b\sigma_1 \otimes \sigma_1\right]. \tag{3.71}$$

Positivity again constraints a, b to the disc $a^2 + b^2 \leq 1$ in the $(\sigma_3 \otimes \sigma_0, \sigma_1 \otimes \sigma_1)$ plane.

The intersection between these two comprises the one-parameter family of X-states

$$\hat{\rho}_{AB} = \frac{1}{4}\left[\sigma_0 \otimes \sigma_0 + b\sigma_1 \otimes \sigma_1\right], \quad -1 \leq b \leq 1. \tag{3.72}$$

But these are *not the only* two-way zero discord states, and this fact is significant in the

light of [207]. To see this, note that in deriving the canonical form (3.69) we assumed $\beta \neq 0$. So we now consider the case $\beta = 0$, so that (3.66) reads

$$\hat{\rho}_{AB} = p_1|0\rangle\langle 0| \otimes \hat{\rho}_{B1} + p_2|1\rangle\langle 1| \otimes \hat{\rho}_{B2}. \tag{3.73}$$

The demand that this be an X-state forces $\hat{\rho}_{AB}$ to be diagonal in the computational basis:

$$\hat{\rho}_{AB}(\{p_{k\ell}\}) = \sum_{k,\ell=0}^{1} p_{k\ell}\, |k\rangle\langle k| \otimes |\ell\rangle\langle \ell|. \tag{3.74}$$

It is manifest that all X-states of this three-parameter family, determined by probabilities $\{p_{k\ell}\}$, $\sum p_{k\ell} = 1$ and worth a *tetrahedron* in extent have vanishing quantum discord and, indeed, vanishing two-way quantum discord.

The intersection of (3.69) and (3.71) given in (3.72) is not really outside the tetrahedron (3.74) in the canonical form because it can be diagonalized by a local unitary $U_A \otimes U_B$, $U_A = U_B = \exp[-i\pi\sigma_2/4]$:

$$\sigma_0 \otimes \sigma_0 + b\sigma_1 \otimes \sigma_1 \rightarrow \sigma_0 \otimes \sigma_0 + b\sigma_3 \otimes \sigma_3. \tag{3.75}$$

Stated differently, the family of strictly one-way zero discord X-states in the canonical form is not a disc, but a disc with the diameter removed.

Remark: Strictly speaking, this is just an half disc with diameter removed, as seen from the fact that in (3.69), (3.71), and (3.72) the two states (a, b), $(a, -b)$ are local unitarily equivalent under $U_A \otimes U_B = \sigma_3 \otimes \sigma_3$. ■

We now consider the correlation ellipsoids associated with these zero discord states. For the one-way zero discord states in (3.71) the non-zero Mueller matrix entries are

$$m_{30} = a, \quad m_{11} = b. \tag{3.76}$$

This ellipsoid is actually a symmetric line segment parallel to the x-axis, of extent $2b$, translated by extent a, perpendicular to the line segment (i.e., along z): $\{(x,y,z) = (x,0,a)| -b \leq x \leq b\}$; it is symmetric under reflection about the z-axis. For measurements on the A side we have from (3.69)

$$m_{03} = a, \;\; m_{11} = b, \tag{3.77}$$

and we get the same line segment structure (recall that now we have to consider M^T in place of M).

For the two-way zero discord states (3.74) we have

$$\begin{aligned} m_{03} &= p_{00} - p_{01} + p_{10} - p_{11}, \\ m_{30} &= p_{00} + p_{01} - p_{10} - p_{11}, \\ m_{33} &= p_{00} - p_{01} - p_{10} + p_{11}, \end{aligned} \tag{3.78}$$

corresponding to a point in the tetrahedron. We note that the associated correlation ellipsoid is a line segment of a diameter *shifted along the diameter itself*. That is, the line segment is radial. While the extent of the line segment and the shift are two parameters, the third parameter is the image I of the maximally mixed input, which does not contribute to the 'shape' of the ellipsoid, but does contribute to the shape. This three parameter family should be contrasted with the claim of [207] that an 'X-state is purely classical if and only if $\hat{\rho}_{AB}$ has components along $\sigma_0 \otimes \sigma_0, \sigma_1 \otimes \sigma_1$' implying a one-parameter family.

3.10 States not requiring an optimization

We now exhibit a large class of states for which one can write down *analytic expression* for quantum discord by inspection, without the necessity to perform explicit optimization over all measurements. We begin by first giving a geometric motivation for this class of

states. Consider X-states for which the associated correlation ellipsoid is *centered at the origin*:

$$z_c = \frac{m_{30} - m_{03}m_{33}}{1 - m_{03}^2} = 0,$$

$$\text{i.e.,} \quad m_{30} = m_{03}m_{33}. \tag{3.79}$$

This implies on the one hand that only two of the three parameters m_{03}, m_{30}, m_{33} are independent. On the other hand, it implies that the product of m_{03}, m_{30}, m_{33} is necessarily positive and thus, by local unitary, all the three can be assumed to be positive without loss of generality. Let us take $m_{03} = \sin\theta > 0$, then we have $m_{30} = m_{33} \sin\theta$. So, we now have in the canonical form a four-parameter family of Mueller matrices

$$M(\gamma_1, \gamma_2, \gamma_3; \theta) = \begin{bmatrix} 1 & 0 & 0 & \sin\theta \\ 0 & \gamma_1 \cos\theta & 0 & 0 \\ 0 & 0 & \gamma_2 \cos\theta & 0 \\ \gamma_3 \sin\theta & 0 & 0 & \gamma_3 \end{bmatrix}, \tag{3.80}$$

and correspondingly a three-parameter family of correlation ellipsoids centered at the origin, with principal axes $(a_x, a_y, a_z) = (\gamma_1, |\gamma_2|, \gamma_3)$, and $z_I = \gamma_3 \sin\theta$. We continue to assume $|\gamma_2| \leq \gamma_1$.

Remark: Note that we are not considering the case of Bell-diagonal states, which too correspond to ellipsoids centered at the origin. In the Bell-diagonal case, the point I is located at the origin and, as an immediate consequence, $S^A_{\min}$ is entirely determined by the major axis of the ellipsoid. In the present case, $z_I = \gamma_1 \cos\theta \neq 0$, and $S^A_{\min}$ does depend on z_I. Indeed, the case of Bell-diagonal states corresponds to $\sin\theta = 0$, and hence what we have here is a one-parameter generalization. ■

The four parameter family of density matrices corresponding to Eq. (3.80) takes the form

$$\rho(\gamma_1, \gamma_2, \gamma_3; \theta) = \frac{1}{4}\begin{bmatrix} (1+\gamma_3)(1+\sin\theta) & 0 & 0 & (\gamma_1+\gamma_2)\cos\theta \\ 0 & (1-\gamma_3)(1-\sin\theta) & (\gamma_1-\gamma_2)\cos\theta & 0 \\ 0 & (\gamma_1-\gamma_2)\cos\theta & (1-\gamma_3)(1+\sin\theta) & 0 \\ (\gamma_1+\gamma_2)\cos\theta & 0 & 0 & (1+\gamma_3)(1-\sin\theta) \end{bmatrix}. \tag{3.81}$$

The first CP condition (3.15) reads

$$\begin{aligned} &(1+\gamma_3)^2 - \sin^2\theta(1+\gamma_3)^2 \geq (\gamma_1+\gamma_2)^2\cos^2\theta, \\ &\text{i.e.,}\ \ \gamma_1+\gamma_2-\gamma_3 \leq 1, \end{aligned} \tag{3.82}$$

while the second CP condition (3.16) reads

$$\begin{aligned} &(1-\gamma_3)^2 - \sin^2\theta(1-\gamma_3)^2 \geq (\gamma_1-\gamma_2)^2\cos^2\theta \\ &\text{i.e.,}\ \ \gamma_1+\gamma_3-\gamma_2 \leq 1. \end{aligned} \tag{3.83}$$

Recalling that $|\gamma|_2 \leq \gamma_1$, these two conditions can be combined into a *single CP condition*

$$\gamma_1 + |\gamma_3 - \gamma_2| \leq 1. \tag{3.84}$$

Having given a full characterization of the centered X-states, we note a special property of these states in respect of quantum discord.

Remark: As seen from Eq. (3.36), the optimal POVM for a centered X-state is a von Neumann measurement since the two curves $a^H(a_z, 0)$ and $a^V(a_z, 0)$ equal a_z. Therefore, the measurement is along x or z according as $a_x > a_z$ or $a_z > a_x$.

Circular states: This special case corresponds to $a_x = a_z$, i.e., setting $\gamma_3 = \gamma_1$ in Eq. (3.80). For this class of states, every von Neumann measurement in the x-z plane (in-

deed, every POVM with all the measurement elements lying in the x-z plane) is equally optimal. In other words, I plays no role in determining the optimal POVM for a centered X-state.

The four eigenvalues of $\hat{\rho}(\gamma_1,\, \gamma_2;\, \theta)$ of (3.81) are

$$\begin{aligned} \{\lambda_j\} &= \frac{1}{4}\{1 + \epsilon\gamma_1 \pm y\}\,, \\ y &= \sqrt{(1+\epsilon\gamma_1)^2\cos^2\theta + (\gamma_1+\epsilon\gamma_2)^2\sin^2\theta}, \end{aligned} \tag{3.85}$$

ϵ being a signature.

We can explicitly write down the various quantities of interest in respect of the circular states $\hat{\rho}(\gamma_1, \gamma_2; \theta)$. First, we note that the conditional entropy post measurement is simply the entropy of the output states that are on the circle, and hence

$$S^A_{\min} = S_2(m_{33}) = S_2(\gamma_1). \tag{3.86}$$

By Eqs. (3.21) and (3.22), we have

$$\begin{aligned} I(\hat{\rho}(\gamma_1,\, \gamma_2;\, \theta)) &= S_2(\gamma_1\, \sin\theta) + S_2(\sin\theta) - S(\{\lambda_j\}), \\ C(\hat{\rho}(\gamma_1,\, \gamma_2;\, \theta)) &= S_2(\gamma_1\, \sin\theta) - S_2(\gamma_1), \\ D(\hat{\rho}(\gamma_1,\, \gamma_2;\, \theta)) &= S_2(\sin\theta) + S_2(\gamma_1) - S(\{\lambda_j\}), \end{aligned} \tag{3.87}$$

where $\lambda_j \equiv \lambda_j(\gamma_1,\, \gamma_2;\, \theta)$ are given in Eq. (3.85). Finally, we note that with the local unitary freedom, this 3-parameter class of states can be lifted to a 9-parameter using local unitaries.

Spherical states: The correlation ellipsoid corresponding to these states is a sphere with $z_c = 0$. They can be obtained as a subset of circular states by setting $\gamma_1 = |\gamma_2|$. The expressions for the correlation are the same as those of circular states as given in Eq. (3.87).

We note that, the spherical states form a 2-parameter family of states inside the set of X-states. We can lift this family to a seven parameter family of states, the five parameters coming from the local unitary transformations. One parameter was however lost from the degeneracy $m_{11} = |m_{22}|$ for spherical states.

Bell mixtures: The next example of a convex combination of the Bell-states was considered in [219]. We can write the state as $\hat{\rho} = \sum_{j=1}^{4} p_j |\phi_j\rangle\langle\phi_j|$, i.e.,

$$\hat{\rho} = \frac{1}{2}\begin{pmatrix} p_1+p_2 & 0 & 0 & p_1-p_2 \\ 0 & p_3+p_4 & p_3-p_4 & 0 \\ 0 & p_3-p_4 & p_3+p_4 & 0 \\ p_1-p_2 & 0 & 0 & p_1+p_2 \end{pmatrix}. \tag{3.88}$$

The corresponding Mueller matrix is diagonal with

$$\begin{aligned} m_{11} &= p_1 + p_3 - (p_2 + p_4), \\ m_{22} &= p_1 + p_4 - (p_2 + p_3), \\ m_{33} &= p_1 + p_2 - (p_3 + p_4). \end{aligned} \tag{3.89}$$

The correlation ellipsoid has $z_c = 0$, and more importantly, $z_I = 0$. The optimal measurement is then a von Neumann projection along the direction of the longest axis length of the ellipsoid.

Linear states: Another example of states for which the quantum discord can be immediately written down are states for which x-z cross-section of the correlation ellipsoid is a line segment along the x-axis. We denote these states as linear states and they are obtained

by setting $a_z = 0$. We have

$$m_{33} = m_{03}m_{30}. \tag{3.90}$$

As before we see that only two of them can have a negative value which can be dropped by a local unitary transformation. This gives us a four parameter family of states for which the optimal measurement is the horizontal entropy. We make the following choice :

$$M(\gamma_1, \gamma_2, \gamma_3, \theta) = \begin{bmatrix} 1 & 0 & 0 & \sin\theta \\ 0 & \gamma_1 \cos\theta & 0 & 0 \\ 0 & 0 & \gamma_2 \cos\theta & 0 \\ \gamma_3 & 0 & 0 & \gamma_3 \sin\theta \end{bmatrix}, \tag{3.91}$$

where we assume $|\gamma_2| < \gamma_1$. Then the CP conditions demand that $\gamma_1 + |\gamma_2| \leq \sqrt{1-\gamma_3^2}$. So we have $|\gamma_2| \leq \min(\gamma_1, \sqrt{1-\gamma_3^2} - \gamma_1)$.

3.11 Conclusions

We develop an optimal scheme for computation of the quantum discord for any X-state of a two-qubit system. Our treatment itself is both comprehensive and self-contained and, moreover, it is geometric in flavour. We exploit symmetry to show, without loss of generality, that the problem itself is one of *optimization over just a single variable*. The analysis is entirely based on the output or correlation ellipsoid.

The optimal measurement is shown to be a three-element POVM. Further, it emerges that the region where the optimal measurement comprises three elements is a tiny wedge shaped one in a slice of the parameter space. On either side of this wedge shaped region one has a von Neumann measurement along the z or x axis as the optimal measurement.

Not all parameters of a two-qubit X-state influence the correlation ellipsoid. The parame-

ters that influence and those which do not influence play very different roles. The correlation ellipsoid has an invariance group which is much larger that the group of local unitary symmetries and comprises of three components. These symmetries are the Lorentz group, another copy of the Lorentz group obtained by the action of spatial inversion, and finally, a scale factor. An appreciation of this larger invariance turns out to be essential to the simplification of the present analysis. We bring out in a transparent manner how the various parameters of the ellipsoid affect the optimal measurement scheme and also provide many examples to demonstrate the same. We also bring out the role played by the partial transpose test at the level of the correlation ellipsoid in respect of entanglement.

Having set up and studied the properties of the optimal measurement, we clearly underline the fact that the region where the assertion of Ali *et al.* is numerically misplaced is really tiny. But the X-states in this tiny region have *the same symmetry* as those outside, perhaps implying that if the symmetry argument of Ali *et al.* is misplaced it is likely to be so everywhere, and not just in this region. We bring out all the above aspects with a useful example.

Finally, we provide numerous examples of states for which the quantum discord can be computed without an explicit optimization problem. These include states with vanishing discord and states whose correlation ellipsoid is centered at the origin.

Appendix : Matrix elements of ρ and M

Matrix elements of ρ_{AB} in terms of the Mueller matrix elements is given by :

$$\rho_{AB} = \frac{1}{4}\left[\begin{array}{c|c|c|c} m_{00}+m_{03}+m_{30}+m_{33} & m_{01}+im_{02}+m_{31}+im_{32} & m_{10}-im_{20}+m_{13}-im_{23} & m_{11}+im_{12}-im_{21}+m_{22} \\ \hline m_{01}-im_{02}+m_{31}-im_{32} & m_{00}-m_{03}+m_{30}-m_{33} & m_{11}-im_{12}-im_{21}-m_{22} & m_{10}-im_{20}-m_{13}+im_{23} \\ \hline m_{10}+im_{20}+m_{13}+im_{23} & m_{11}+im_{12}+im_{21}-m_{22} & m_{00}+m_{03}-m_{30}-m_{33} & m_{01}+im_{02}-m_{31}-im_{32} \\ \hline m_{11}-im_{12}+im_{21}+m_{22} & m_{10}+im_{20}-m_{13}-im_{23} & m_{01}-im_{02}-m_{31}+im_{32} & m_{00}-m_{03}-m_{30}+m_{33} \end{array}\right],$$

and that of M in terms of ρ_{AB} by :

$$M = \left[\begin{array}{c|c|c|c} 1 & \rho_{01}+\rho_{10}+\rho_{23}+\rho_{32} & -i[(\rho_{01}-\rho_{10})+(\rho_{23}+\rho_{32})] & (\rho_{00}-\rho_{11})+(\rho_{22}-\rho_{33}) \\ \hline \rho_{02}+\rho_{20}+\rho_{13}+\rho_{31} & \rho_{03}+\rho_{30}+\rho_{12}+\rho_{21} & -i[(\rho_{03}-\rho_{12})+(\rho_{21}-\rho_{30})] & \rho_{02}+\rho_{20}-(\rho_{13}+\rho_{31}) \\ \hline i[(\rho_{02}-\rho_{20})+(\rho_{13}-\rho_{31})] & i[(\rho_{03}+\rho_{12})-(\rho_{21}+\rho_{30})] & \rho_{30}+\rho_{03}-(\rho_{12}+\rho_{21}) & i[(\rho_{02}-\rho_{20})-(\rho_{13}-\rho_{31})] \\ \hline \rho_{00}+\rho_{11}-(\rho_{22}+\rho_{33}) & \rho_{01}+\rho_{10}-(\rho_{23}+\rho_{32}) & -i[(\rho_{01}-\rho_{10})-(\rho_{23}-\rho_{32})] & \rho_{00}+\rho_{33}-(\rho_{11}+\rho_{22}) \end{array}\right]. \tag{3.92}$$